


PAPER

# Early warning signs for SPDEs with continuous spectrum

Paolo Bernuzzi<sup>1</sup> , Antonia Freya Susanne Dux<sup>1</sup> and Christian Kuehn<sup>1,2</sup>

<sup>1</sup>Department of Mathematics, School of Computation Information and Technology, Technical University of Munich, Garching 85748, Germany

<sup>2</sup>Munich Data Science Institute, Technical University of Munich, Garching 85748, Germany

**Corresponding author:** Paolo Bernuzzi; Email: [paolo.bernuzzi@ma.tum.de](mailto:paolo.bernuzzi@ma.tum.de)

**Received:** 27 July 2023; **Revised:** 27 February 2024; **Accepted:** 07 July 2024

**Keywords:** early warning signs; SPDEs; scaling law; continuous spectrum; multiplication operator

**2020 Mathematics Subject Classification:** 60H15 (Primary); 35R60, 65C30, 47A11 (Secondary)

## Abstract

In this work, we study early warning signs for stochastic partial differential equations (SPDEs), where the linearisation around a steady state is characterised by continuous spectrum. The studied warning sign takes the form of qualitative changes in the variance as a deterministic bifurcation threshold is approached via parameter variation. Specifically, we focus on the scaling law of the variance near the transition. Since we are dealing here, in contrast to previous studies, with the case of continuous spectrum and quantitative scaling laws, it is natural to start with linearisations of the drift operator that are multiplication operators defined by analytic functions. For a one-dimensional spatial domain, we obtain precise rates of divergence. In the case of the two- and three-dimensional domains, an upper bound to the rate of the early warning sign is proven. These results are cross-validated by numerical simulations. Our theory can be generically useful for several applications, where stochastic and spatial aspects are important in combination with continuous spectrum bifurcations.

## 1 Introduction

Solutions of various complex systems and differential equations with multiple time scales are known to display critical transitions [41]. After a longer period of slow change, a critical transition corresponds to a large/dramatic event happening on a fast scale. In more detail, we can characterise this mechanism [39, 43] by several essential components. The typical dynamics of such systems display slow motion for long times. Yet, there is generically a slow drift towards a bifurcation point of the fast/layer subsystem. The critical transition is an abrupt change that happens on a fast timescale after the bifurcation point has been passed. Of course, it is of interest to study whether there are early warning signs to potentially anticipate a critical transition. One crucial mechanism to extract warning signs from data is to exploit the effect of critical slowing down, where the recovery of perturbations to the current state starts to slow as a bifurcation is approached. This behaviour can therefore be observed in real-life data by exploiting natural fluctuations caused by minor physical components, treated as stochastic perturbation effects and by measuring a stochastic observable, such as variance or autocorrelation [65]. This approach has recently gained considerable popularity in various applications [58].

It is evident that in many complex systems with critical transitions, we should also take into account, beyond stochasticity, the spatial components. A prime example are applications in neuroscience, where it is apparent that larger-scale events, such as epileptic seizures, can be described by spatial stochastic systems with critical transitions [49, 50, 53]. Another example is electric power systems where critical transitions can lead to a failure of the whole system, such as voltage collapses [14]. Other examples of



complex systems with critical transitions occur in medical applications [55, 63], economic applications [48] and environmental applications [1, 46, 59]. It becomes apparent that for each of these applications, a prediction and warning of a critical transition is desirable as it could enable the prevention of its occurrence or at least improve the adaptability to it. Yet, to make early warning sign theory reliable and avoid potential non-robust conclusions [17, 20], a rigorous mathematical study of early warning sign theory is needed. There exists already a quite well-developed theory for warning signs of systems modeled by stochastic ordinary differential equations (SODE), for example in [15, 40]. However, there are still many open problems for systems modeled by stochastic partial differential equations (SPDE). For SPDEs, it is potentially even more crucial in comparison to SODEs to develop a mathematical theory as SPDEs model complex systems, where it is either extremely costly to obtain high-resolution experimental, or even simulation, data in many applications. Therefore, experimentally driven approaches have to be guided by rigorous mathematical analysis.

For our study, we follow the construction in [43], which considers differential equations of the form

$$\begin{cases} du(x, t) = (F_1(x, p(t))u(x, t) + F_2(u(x, t), p(t))) dt + \sigma dW(t), \\ dp(t) = \epsilon G(u(x, t), p(t)) dt, \end{cases} \quad (1.1)$$

with  $(x, t) \in \mathcal{X} \times [0, \infty)$  for a connected set  $\mathcal{X} \subseteq \mathbb{R}^N$  with nonempty interior,  $u: \mathcal{X} \times [0, \infty) \rightarrow \mathbb{R}$ ,  $p: [0, \infty) \rightarrow \mathbb{R}$  and  $N \in \mathbb{N} := \{1, 2, 3, \dots\}$ . Suppose that  $F_1$  is a linear operator and that  $F_2$  and  $G$  are sufficiently smooth nonlinear maps. We assume  $\sigma > 0$ ,  $0 < \epsilon \ll 1$  and with the notation  $W$  we refer to a  $Q$ -Wiener process. The precise properties of the operator  $Q$  are described further below. We denote  $u(x, t)$  by  $u$  and  $p(t)$  as  $p$ .

Suppose, for simplicity, that  $F_2(0, p) = 0$ . Hence, we obtain for any  $p$  the homogeneous steady state  $u_* \equiv 0$  for the deterministic partial differential equation (PDE) corresponding to (1.1) with  $\sigma = 0$ . To determine the local stability of  $u_* \equiv 0$ , we study the linear operator

$$A(p) := F_1 + D_{u_*} F_2(0, p),$$

where  $D_{u_*}$  is the Fréchet derivative of  $u$  on a suitable Banach space, which contains the solutions of (1.1) and which is described in full detail below.

Suppose that the spectrum of  $A(p_0)$  is contained in  $\{z: \operatorname{Re}(z) < 0\}$  for fixed values  $p_0 < 0$ , whereas the spectrum has elements in  $\{z: \operatorname{Re}(z) > 0\}$  for fixed  $p_0 > 0$ . Therefore, the fast subsystem, given by taking the limit  $\epsilon = 0$ , has a bifurcation point at  $p = 0$  and in the full fast-slow system (1.1), with  $\epsilon > 0$ , the slow dynamics  $\partial_t p = \epsilon G(0, p)$  can drive the system to the bifurcation point at  $p = 0$  and potentially induce a critical transition. For the case  $\epsilon = 0$ , the variable  $p$  becomes a parameter on which the motion of  $u$  depends. More precisely, as  $p$  is varying, it can cross the bifurcation threshold  $p = 0$  present in the fast PDE dynamics  $\partial_t u = F_1 u + F_2(u, p)$ . As of now, we consider for simplicity the case  $\epsilon = 0$  and assume that  $p$  is a parameter (see [23] for steps towards a more abstract theory of fast-slow SPDEs). The problem studied is hence of the form of the fast system linearised at  $u_*$ ,

$$dU(x, t) = A(p)U(x, t) dt + \sigma dW(t). \quad (1.2)$$

For  $p \ll 0$  and initial condition in  $u_*$ , the dissipative linear term constrains the solution of such a system and the solution of (1.1) at  $\epsilon = 0$  in a neighbourhood of  $u_*$  with high probability. Therefore the two paths are expected to present a similar behaviour and variance [24]. The observation of an early warning sign on the linearised system is therefore justified up to proximity to the bifurcation threshold. We discuss this problem setting initially  $A(p) = pI + T_f$ , where  $I$  denotes the identity and  $T_f$  is a multiplication operator associated to a function  $f: \mathcal{X} \rightarrow \mathbb{R}$ . Such a choice is directly motivated by the spectral theorem [25], which associates a multiplication operator with other operators with the same spectrum. For the precise technical set-up and assumptions made, we refer to Section 2. Generalisations to the choice of operator  $A(p)$  are discussed in Section 5 and, from an applied perspective, in Section 7.

As mentioned above, prediction of critical transitions is very important in applications as it can help reduce, or even completely evade, its effects. This can be done by finding early warning signs [5, 7]. Our goal is to analyse the problem for early warning signs in the form of an increasing variance as the bifurcation point at  $p = 0$  is approached.

This paper is structured as follows. In Section 2, we set up the problem and state our main results. In Section 3, we discuss the variance of the solutions of (1.2) for measurable functions  $f$  that are defined on a one-dimensional space, i.e., assuming that  $N = 1$ . We first focus on a specific tool function type and then generalise the obtained results to the case of more general analytic functions. In Section 4, we proceed with the study of the scalar product that defines the variance along certain directions in the space of square-integrable functions, with the domain of  $f$  in higher dimensions. While observing convergence as  $p \rightarrow 0^-$  for  $N > 1$  dimensions and  $f$  under certain assumptions, we further find an upper bound of divergence for analytic functions  $f$  on two- and three-dimensional domains. In Section 5, we discuss how our results are affected by relaxing certain assumptions and we provide examples of the effectiveness of the early warning-signs for different types of linear operators presented in the drift term of (1.2). In Section 6, we approximate (1.2) for one-, two- and three-dimensional spatial domains to obtain visual numerical representations and a cross-validation of the discussed theorems. Lastly, in Section 7, we provide examples of models employed in various research fields on which the early warning signs find application.

## 2 Preliminaries

In this paper, we study the SPDE

$$\begin{cases} du(x, t) = (f(x) + p) u(x, t) dt + \sigma dW(t) \\ u(\cdot, 0) = u_0 \end{cases} \tag{2.1}$$

for  $x \in \mathcal{X}, t > 0$  and  $\mathcal{X} \subseteq \mathbb{R}^N$  a connected set with non-empty interior for  $N \in \mathbb{N}$ . The operator  $T_f$  denotes the realisation in  $L^2(\mathcal{X})$  of the multiplication operator for  $f$ , i.e.

$$T_f u = fu \quad , \quad \mathcal{D}(T_f) := \left\{ u \text{ Lebesgue measurable} \mid fu \in L^2(\mathcal{X}) \right\} \quad ,$$

with  $\mathcal{D}(\cdot)$  denoting the domain of an operator. We assume that the initial condition of the system satisfies  $u_0 \in \mathcal{D}(T_f)$  and  $L^2(\mathcal{X})$  is the Hilbert space of square-integrable functions with the standard scalar product  $\langle \cdot, \cdot \rangle$ . We denote as  $\mathcal{H}^s(\mathcal{X})$  the Hilbert Sobolev space of degree  $s$  on  $\mathcal{X}$ . We are going to assume that the Lebesgue measurable function  $f : \mathcal{X} \rightarrow \mathbb{R}$  satisfies

$$f(x) < 0 \quad \forall x \in \mathcal{X} \setminus \{x_*\}, \quad \int_{\mathcal{X}} \frac{1}{|f(x) - p|} dx < +\infty \text{ for any } p < 0, \text{ and } f(x_*) = 0, \tag{2.2}$$

for a point  $x_* \in \mathcal{X}$ . Without loss of generality, i.e., up to a translation coordinate change in space, we can set  $x_* = 0$ , where 0 denotes the origin in  $\mathbb{R}^N$ . We can then assume, again using a translation of space, that there exists  $\delta > 0$  such that  $[0, \delta]^N \subseteq \mathcal{X}$ . We assume also  $\sigma > 0$  and  $p < 0$ .

The construction of the noise process  $W$  and the existence of the solution follow from standard methods [16] as follows. For fixed  $T > 0$ , we consider the probability space  $(\Omega, \mathcal{F}, \mathbb{P})$  with  $\Omega$  the space of paths  $\{X(t)\}_{t \in [0, T]}$  such that  $X(t) \in L^2(\mathcal{X})$  for any  $t \in [0, T]$ , for  $\mathcal{F}$  the Borel  $\sigma$ -algebra on  $\Omega$  and with  $\mathbb{P}$  a Wiener measure induced by a Wiener process on  $[0, T]$ . To this probability space, we associate the natural filtration  $\mathcal{F}_t$  of  $\mathcal{F}$  with respect to a Wiener process for  $t \in [0, T]$ .

We consider the non-negative operator  $Q : L^2(\mathcal{X}) \rightarrow L^2(\mathcal{X})$  with eigenvalues  $\{q_k\}_{k \in \mathbb{N}}$  and eigenfunctions  $\{b_k\}_{k \in \mathbb{N}}$ . For  $Q$  assumed to be trace class, the stochastic process  $W$  is called  $Q$ -Wiener process if

$$W(t) = \sum_{i=1}^{\infty} \sqrt{q_i} b_i \beta^i(t) \tag{2.3}$$

holds for a family  $\{\beta^i\}_{i \in \mathbb{N}}$  of independent, identically distributed and  $\mathcal{F}_t$ -adapted Brownian motions. Such series converges in  $L^2(\Omega, \mathcal{F}, \mathbb{P})$  by [16, Proposition 4.1]. Throughout the paper, we assume  $Q$  to be a self-adjoint bounded operator. In this case, there exists a larger space ([16, Proposition 4.11]), denoted by  $H_1$ , on which  $Q^{\frac{1}{2}}L^2(\mathcal{X})$  embeds through a Hilbert–Schmidt operator and such that the series in (2.3) converges in  $L^2(\Omega, \mathcal{F}, \mathbb{P}; H_1)$ . The resulting stochastic process  $W$  is called a generalised Wiener process.

Assuming  $u_0$  to be  $\mathcal{F}_0$ -measurable, properties (2.2) imply that there exists a unique mild solution for the system (2.1) of the form

$$u(\cdot, t) = e^{(f(\cdot)+p)t}u_0 + \sigma \int_0^t e^{(f(\cdot)+p)(t-s)} dW(s) \quad ,$$

with  $t > 0$ , as stated by [16, Theorem 5.4]. From [16, Theorem 5.2], we can obtain the covariance operator of the mild solution of (2.1) as

$$V(t) := \sigma^2 \int_0^t e^{T_{f+p} s} Q e^{T_{f+p} s} ds$$

for any  $t > 0$ . We also define  $V_\infty := \lim_{t \rightarrow \infty} V(t)$ , which is the operator that is used to construct the discussed early warning signs, i.e., we are interested in the scaling laws that the covariance operator can exhibit as we vary the parameter  $p$  towards the bifurcation point at  $p = 0$ .

We employ the big theta notation [35],  $\Theta$ , in the limit to 0, i.e.  $b_1 = \Theta(b_2)$  if  $\lim_{s \rightarrow 0} \frac{b_1(s)}{b_2(s)}, \lim_{s \rightarrow 0} \frac{b_2(s)}{b_1(s)} > 0$  for  $b_1$  and  $b_2$  locally positive functions. The direction along which such a limit is approached is indicated by the space on which the parameter is defined.

### 2.1 Results

We primarily set  $Q = I$ , the identity operator on  $L^2(\mathcal{X})$ . The definition of  $V_\infty$  implies, through Fubini’s Theorem, that

$$\begin{aligned} \langle g_1, V_\infty g_2 \rangle &= \int_{\mathcal{X}} g_1(x) \sigma^2 \lim_{t \rightarrow \infty} \int_0^t e^{(f(x)+p)r} Q e^{(f(x)+p)r} g_2(x) dr dx \\ &= \int_{\mathcal{X}} g_1(x) g_2(x) \frac{-\sigma^2}{2(f(x) + p)} dx = \frac{\sigma^2}{2} \left\langle \frac{-1}{f + p} g_1, g_2 \right\rangle, \end{aligned} \tag{2.4}$$

with  $g_1, g_2 \in L^2(\mathcal{X})$ . We set  $g_1 = g_2 = g$  and, initially, we take  $g = \mathbb{1}_{[0, \varepsilon]^N}$  or  $g = \mathbb{1}_{[-\varepsilon, \varepsilon]^N}$  for small enough  $\varepsilon > 0$ . These indicator functions allow us to understand the scaling laws near the bifurcation point analytically as they are localised near the zero of  $f$  at  $x_* = 0$ . More general classes of test functions for the inner product with  $V_\infty$  can then be treated in the usual way via approximation with simple functions.

In Section 3, Theorem 3.3 provides the scaling law of  $\langle g, V_\infty g \rangle$  for  $N = 1$  and for an analytic function  $f : \mathcal{X} \rightarrow \mathbb{R}$ . Similarly, in Section 4, Theorem 4.5 and Theorem 4.7 provide an upper bound for the rate of divergence of  $\langle g, V_\infty g \rangle$  for  $N = 2$  and  $N = 3$  respectively. Further, similar results are obtained under relaxed assumptions in Section 5 on  $g$ , the operator  $Q$  and the linear operator present in the drift component of (2.1). Moreover, Section 6 provides plots that cross-validate the stated conclusions through the implicit Euler–Maruyama method and computation of the integrals occurring in the mentioned theorems. Lastly, in Section 7, applications to the obtained results are examined.

### 3 One-dimensional case

In the current section, we assume  $N = 1$  and obtain a precise rate of divergence of the time-asymptotic variance of the solution of (2.1) for different types of functions  $f : \mathcal{X} \subseteq \mathbb{R} \rightarrow \mathbb{R}$ . Such a behaviour defines an early warning sign that precedes a bifurcation threshold of the system as  $p$  approaches 0 from below.

First, we choose a specific function type  $f$  to analyse. Afterwards, we expand our analysis by considering general analytic functions and, lastly, we discuss an example in which  $f$  is not analytic.

**Table 1.** Scaling law of the time-asymptotic variance in dimension  $N = 1$  for the function  $f = f_\alpha(x)$  and  $g = \mathbb{1}_{[0,\varepsilon]}$

Case	Scaling law for $p \rightarrow 0^-$
$0 < \alpha < 1$	1
$\alpha = 1$	$-\log(-p)$
$\alpha > 1$	$(-p)^{-1+\frac{1}{\alpha}}$
$\alpha \rightarrow \infty$	$(-p)^{-1}$

### 3.1 Tool function

Consider the function  $f_\alpha$  defined by

$$f_\alpha(x) := -|x|^\alpha \quad \text{with } \alpha > 0 \tag{3.1}$$

with  $x$  in a neighbourhood of  $x_* = 0$  and such that (2.2) holds. This type of function is a useful tool for the study of system (2.1). Indeed, for  $f$  such that there exist  $c_1, c_2, \varepsilon > 0$  and

$$c_1 f_\alpha(x) \leq f(x) \leq c_2 f_\alpha(x) \quad \forall x \in [-\varepsilon, \varepsilon] \cap \mathcal{X}, \tag{3.2}$$

we may transfer scaling laws obtained from the tool function directly to results for  $f$ . We note that up to rescaling of the spatial variable, we can assume  $\varepsilon = 1$  and that  $[0, 1] \subseteq \mathcal{X}$ . Hence, using  $T_{f_\alpha}$  to analyse the covariance operator and by (2.4) we obtain

$$\langle g, V_\infty g \rangle = - \left\langle g, \frac{\sigma^2}{2(f(x) + p)} g \right\rangle = \int_0^1 \frac{\sigma^2}{2(-f(x) - p)} dx$$

and

$$\frac{1}{2c_1} \int_0^1 \frac{\sigma^2}{x^\alpha - p} dx \leq \int_0^1 \frac{\sigma^2}{2(-f(x) - p)} dx \leq \frac{1}{2c_2} \int_0^1 \frac{\sigma^2}{x^\alpha - p} dx \tag{3.3}$$

for  $g(x) = \mathbb{1}_{[0,1]}$  and certain constants  $c_1 \geq 1 \geq c_2$ .

The following theorem describes the rate of divergence assumed by  $\langle g, V_\infty g \rangle$  as  $p \rightarrow 0^-$  for  $f = f_\alpha$ .

**Theorem 3.1.** For  $f = f_\alpha$  defined in (3.1),  $Q = I$  and  $\varepsilon > 0$ , the time-asymptotic covariance  $V_\infty$  of the solution of (2.1) along  $g(x) = \mathbb{1}_{[0,\varepsilon]}$ ,  $\langle g, V_\infty g \rangle$ , presents scaling law, as  $p \rightarrow 0^-$ , described in Table 1.

**Proof.** The scaling law of  $\langle g, V_\infty g \rangle$  for  $p \rightarrow 0^-$  is equivalent to the one exhibited by  $\int_0^1 \frac{1}{x^\alpha - p} dx$ , as described in (3.3). In such a limit in  $p$  we obtain

$$\lim_{p \rightarrow 0^-} \int_0^1 \frac{1}{x^\alpha - p} dx = \int_0^1 \frac{1}{x^\alpha} dx = \begin{cases} < \infty & \text{for } 0 < \alpha < 1, \\ = \infty & \text{for } \alpha \geq 1. \end{cases}$$

For the case  $\alpha = 1$ , by substituting  $y = x - p$  we find that

$$\int_0^1 \frac{1}{x - p} dx = \int_{-p}^{1-p} \frac{1}{y} dy = \log(1 - p) - \log(-p) = \Theta(-\log(-p)) \quad \text{for } p \rightarrow 0^-.$$

We now consider the case  $\alpha > 1$ . Through the substitution  $y = x(-p)^{-\frac{1}{\alpha}}$  we obtain

$$\int_0^1 \frac{1}{x^\alpha - p} dx = \frac{1}{-p} \int_0^1 \frac{1}{(x(-p)^{-\frac{1}{\alpha}})^\alpha + 1} dx = (-p)^{-1+\frac{1}{\alpha}} \int_0^{(-p)^{-\frac{1}{\alpha}}} \frac{1}{y^\alpha + 1} dy. \tag{3.4}$$

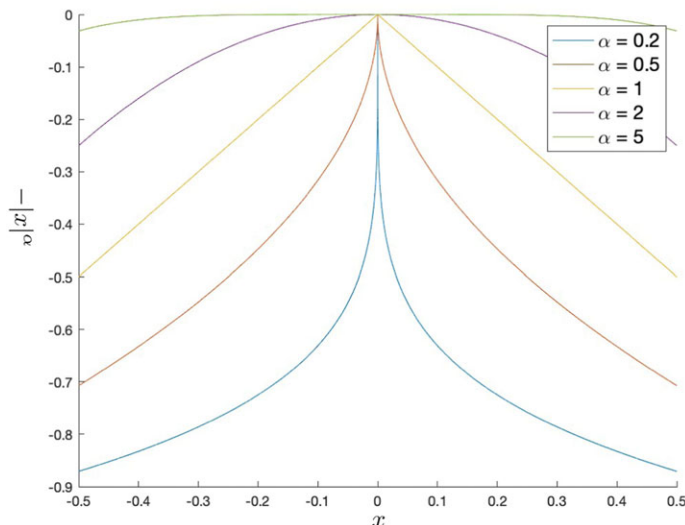


**Figure 1.** Plot of function  $-|x|^\alpha$  for different choices of  $\alpha$ . For  $\alpha > 1$ , the function is  $C^1$ , with derivative equal to 0 at  $x = 0$ , therefore flat in 0. Conversely, for  $\alpha \leq 1$  the function is steep at  $x = 0$ .

Since  $\alpha > 1$ , we find that

$$\lim_{p \rightarrow 0^-} \int_0^{(-p)^{-\frac{1}{\alpha}}} \frac{1}{y^\alpha + 1} dy < \infty. \tag{3.5}$$

Hence, taking the limit in  $p$  to zero from below for the equation (3.4), we find divergence with the rate

$$(-p)^{-1+\frac{1}{\alpha}} \int_0^{(-p)^{-\frac{1}{\alpha}}} \frac{1}{y^\alpha + 1} dy = \Theta\left((-p)^{-1+\frac{1}{\alpha}}\right).$$

Further, we see that, for  $\alpha$  approaching infinity, this expression is also well-defined with rate of divergence  $\Theta\left(\frac{1}{-p}\right)$ . □

Theorem 3.1 states that, for the function  $f_\alpha$  defined by (3.1) and  $0 < \alpha < 1$ , the time-asymptotic variance along  $g$  is converging in the limit  $p \rightarrow 0^-$ . Such function types  $f_\alpha$  display a steep shape on 0, as seen in Figure 1, given by the fact that their left and right first derivative assume infinite values. Alternatively, we observe that for  $\alpha \geq 1$ , the time-asymptotic variance along  $g$  diverges, indicating that a divergence appears as the graph gets flatter and smoother, increasing  $\alpha$ . The intuition behind such difference is given by the fact that, although the solution  $u$  of (2.1) is less affected by the drift component on all  $x \in \mathcal{X}$  as  $p$  approaches 0, the only region in space on which  $u$  is solely driven by noise in the limit case is the set  $\{x_* = 0\}$ . In particular, while the time-asymptotic variance of  $u(x, \cdot)$  increases for all  $x \in \mathcal{X}$ , it presents divergence only on  $x_*$  due to the fact that  $u(x_*, \cdot)$  is the solution of an Orstein–Uhlenbeck equation for any  $p \leq 0$ . Analytically, it appears that for steep shapes of  $f_\alpha$  on  $x_*$ , the divergence of the time-asymptotic variance of  $u(x_*, \cdot)$  does not affect  $\langle g, V_\infty g \rangle$ , as it is restricted by the dissipative effect of the drift component on  $x \in (0, \varepsilon]$ . Conversely, for smooth  $f_\alpha$  on  $x_*$ , the dissipation induced by the multiplication operator on  $u(x, \cdot)$ , for  $x \in (0, \varepsilon]$ , is too weak to imply convergence of  $\langle g, V_\infty g \rangle$ , but affects its rate of divergence. It is interesting to note that a similar scaling law behaviour, associated with the intermittency scaling

law of an ODE dependent on a parameter near a non-smooth fold bifurcation, has been found in [38, Table 1].

**Remark 3.2.** Under the assumptions of Theorem 3.1, the finite time  $t > 0$  variance along a function  $g$ ,  $\langle g, V(t)g \rangle$ , converges for  $p \rightarrow 0^-$ . Up to rescaling of  $x$ , we fix  $\varepsilon = 1$  and note that

$$\begin{aligned} \langle g, V(t)g \rangle &= \int_0^\infty g(x)\sigma^2 \int_0^t e^{(f(x)+p)r} Q e^{(f(x)+p)r} g(x) \, dr \, dx \\ &= -\sigma^2 \int_0^1 \frac{1 - e^{2(f(x)+p)t}}{2(f(x)+p)} \, dx < +\infty \end{aligned}$$

for any  $p \leq 0$ . The growths of finite time variances are, therefore, early warning signs which are hard to observe in finite time series due to the fact that they increase as  $p$  approaches 0 but do not diverge. For any fixed  $p \geq 0$ , longer times  $t$  imply that the variance attains higher values.

### 3.2 General analytic functions

We have found that  $\langle g, V_\infty g \rangle$  converges for  $\alpha < 1$  and diverges for  $\alpha \geq 1$ , with corresponding rate of divergence, for the limit  $p \rightarrow 0^-$  with the functions  $f_\alpha(x) = -|x|^\alpha$  and  $g = \mathbb{1}_{[0,\varepsilon]}$ . Our aim in this subsection is to generalise this result considerably. In particular, we now consider analytic functions  $f$  such that (2.2) holds. Applying Taylor’s theorem and due to the fact that  $f$  vanishes at  $x_* = 0$ , the function  $f$  is of the form

$$f(x) = -\sum_{n=1}^\infty a_n x^n$$

for any  $x \in \mathcal{X}$  and with coefficients  $\{a_n\}_{n \in \mathbb{N}} \subset \mathbb{R}$  such that (2.2) holds. Up to reparametrisation, we assume that  $[0, \varepsilon] \subseteq \mathcal{X}$ . The following theorem provides a scaling law, which can be used as an early warning sign, of the expression  $\langle g, V_\infty g \rangle$  for an analytic  $f$  and  $g(x) = \mathbb{1}_{[0,\varepsilon]}$ .

**Theorem 3.3.** Set  $f(x) = -\sum_{n=1}^\infty a_n x^n$  for all  $x \in \mathcal{X} \subseteq \mathbb{R}$  that satisfies (2.2),  $\{a_n\}_{n \in \mathbb{N}} \subset \mathbb{R}$  and  $Q = I$ . Let  $m \in \mathbb{N}$  denote the index for which  $a_n = 0$  for any  $n \in \{1, \dots, m - 1\}$  and  $a_m \neq 0$ .<sup>1</sup> Then the time-asymptotic variance of the solution of (2.1) along  $g(x) = \mathbb{1}_{[0,\varepsilon]}$ ,  $\langle g, V_\infty g \rangle$ , is characterised by the scaling law, as  $p \rightarrow 0^-$ , described in Table 1, now depending on the value of  $m = \alpha > 0$ .<sup>2</sup>

**Proof.** As in the proof of Theorem 3.1, up to rescaling of the variable  $x$ , we can choose  $\varepsilon = 1$ . Analysing the variance along  $g$ , we obtain that

$$\langle g, V_\infty g \rangle = \frac{\sigma^2}{2} \int_0^1 \frac{1}{\sum_{n=m}^\infty a_n x^n - p} \, dx \quad (3.6)$$

For positive  $x$  close to zero, the sum  $\sum_{n=1}^\infty a_n x^n$  is dominated by the leading term  $a_m x^m$ , since

$$\lim_{x \rightarrow 0^+} \frac{\sum_{n=1}^\infty a_n x^n}{a_m x^m} = \lim_{x \rightarrow 0^+} \frac{\sum_{n=m}^\infty a_n x^n}{a_m x^m} = \lim_{x \rightarrow 0^+} \frac{a_m + \sum_{n=m+1}^\infty a_n x^{n-m}}{a_m} = 1.$$

<sup>1</sup>For odd  $m$  it is implied that  $\mathcal{X} \subseteq \mathbb{R}_{\geq 0} := \{x \in \mathbb{R} : x \geq 0\}$ , or  $\mathcal{X} \subseteq \mathbb{R}_{\leq 0} := \{x \in \mathbb{R} : x \leq 0\}$  up to rescaling, due to the sign of  $f$ .

<sup>2</sup> Alternatively, we can assume to have a function  $f \in C^k$  such that  $k \geq m$ . This leads to the study of the Peano remainder instead of the whole series.

**Table 2.** Scaling law of the time-asymptotic variance in dimension  $N = 1$  for the function  $f = f_\alpha(x)$  and  $g = x^{-\gamma} \mathbb{1}_{[0,\varepsilon]}$

Case	Scaling law for $p \rightarrow 0^-$
$0 < 2\gamma + \alpha < 1$	1
$2\gamma + \alpha = 1$	$-\log(-p)$
$2\gamma + \alpha > 1$	$(-p)^{-1 + \frac{1-2\gamma}{\alpha}}$
$2\gamma \rightarrow 1$ or $\alpha \rightarrow \infty$	$(-p)^{-1}$

Therefore, there exists a constant  $C > 1$  such that for any  $x \in (0, 1]$

$$\frac{1}{C} a_m x^m \leq \sum_{n=1}^{\infty} a_n x^n \leq C a_m x^m$$

holds true. Hence, for (3.6) we obtain

$$\frac{\sigma^2}{C} \int_0^1 \frac{1}{a_m x^m - p} dx \leq \sigma^2 \int_0^1 \frac{1}{\sum_{n=1}^{\infty} a_n x^n - p} dx \leq C \sigma^2 \int_0^1 \frac{1}{a_m x^m - p} dx.$$

This result is equivalent to (3.3), in the sense that it implies that the rate of divergence of  $\langle g, V_\infty g \rangle$  is described in Table 1 with  $m = \alpha$ . □

**Remark 3.4.** In Theorem 3.3, we have considered bounded functions  $g$ . Through similar methods as the proof of Theorem 3.1, a scaling law can be obtained for more general families of functions in  $L^2(\mathcal{X})$ . For example, we consider  $\varepsilon > 0$  such that  $[0, \varepsilon] \subseteq \mathcal{X}$ ,  $g = x^{-\gamma} \mathbb{1}_{[0,\varepsilon]}$ ,  $\gamma < \frac{1}{2}$ ,  $f = f_\alpha$  and  $\alpha > 0$ , which yields

$$\langle g, V_\infty g \rangle = \frac{\sigma^2}{2} \int_0^\varepsilon \frac{1}{x^{2\gamma}} \frac{1}{x^\alpha - p} dx.$$

Hence, for  $0 < 2\gamma + \alpha < 1$ , we obtain

$$\lim_{p \rightarrow 0^-} \langle g, V_\infty g \rangle = \frac{\sigma^2}{2} \int_0^\varepsilon \frac{1}{x^{2\gamma+\alpha}} dx < +\infty.$$

Setting instead  $2\gamma + \alpha \geq 1$ , we get

$$\begin{aligned} \langle g, V_\infty g \rangle &= \frac{\sigma^2}{2} \int_0^\varepsilon \frac{1}{x^{2\gamma}} \frac{1}{x^\alpha - p} dx \\ &= \frac{\sigma^2}{2} (-p)^{-1 + \frac{2\gamma}{\alpha}} \int_0^\varepsilon \frac{1}{(x(-p)^{-\frac{1}{\alpha}})^{2\gamma}} \frac{1}{(x(-p)^{-\frac{1}{\alpha}})^\alpha + 1} dx \\ &= \frac{\sigma^2}{2} (-p)^{-1 + \frac{1-2\gamma}{\alpha}} \int_0^{\varepsilon(-p)^{-\frac{1}{\alpha}}} \frac{1}{y^{2\gamma}} \frac{1}{y^\alpha + 1} dy, \end{aligned}$$

for  $y = x(-p)^{-\frac{1}{\alpha}}$ . The scaling law for  $\langle g, V_\infty g \rangle$  in  $p \rightarrow 0^-$  is summarised in Table 2. This result generalises the statement in [43, Theorem 4.4] as an exact scaling law can be obtained for any analytic  $f$  that satisfies (2.2) and  $g$  in a dense subset of  $L^2(\mathcal{X})$ .

**Remark 3.5.** We found that the scaling law of the time-asymptotic variance, along an indicator function, of the solution of (2.1) is shown in Table 1 for every function  $f$  that satisfies (2.2) and (3.2) for  $\alpha > 0$ . Clearly, this does not include all possible functions  $f$ . We take as an example the case in which there



exists  $\delta \geq 1$  such that  $[-\delta, \delta] \subseteq \mathcal{X}$  and functions  $f$  that converge at two different rates as  $x$  approaches  $0^-$  and  $0^+$ . We consider

$$f(x) = \begin{cases} f_1(x) & \text{for } 0 \geq x \in \mathcal{X}, \\ f_2(x) & \text{for } 0 < x \in \mathcal{X}, \end{cases}$$

for smooth functions  $f_1 : \mathcal{X} \cap \mathbb{R}_{\leq 0} \rightarrow \mathbb{R}$  and  $f_2 : \mathcal{X} \cap \mathbb{R}_{\geq 0} \rightarrow \mathbb{R}$  and  $f$  that satisfies (2.2). We assume  $g(x) = \mathbb{1}_{[-1,1]}(x)$  and by (2.4) we get

$$\langle g, V_\infty g \rangle = \int_{-1}^1 \frac{-\sigma^2}{2(f(x) + p)} dx = \frac{\sigma^2}{2} \int_{-1}^0 \frac{1}{-f_1(x) - p} dx + \frac{\sigma^2}{2} \int_0^1 \frac{1}{-f_2(x) - p} dx. \tag{3.7}$$

We consider each summand separately and take the limit in  $p$  to zero from below. If  $\lim_{x \rightarrow 0^+} f_2(x) < 0$ , then

$$\lim_{p \rightarrow 0^-} \int_0^1 \frac{1}{-f_2(x) - p} dx < +\infty$$

and the scaling rate of  $\langle g, V_\infty g \rangle$  is equivalent to the one given by  $\int_{-1}^0 \frac{1}{-f_1(x) - p} dx$ . Otherwise, it is dictated by the highest rate associated with the two summands. Such rates are shown in Table 1, assuming that  $f_1$  and  $f_2$  are analytic or that they have the same order of convergence to 0 as  $f_\alpha$  for any  $\alpha > 0$ .

### 4 Higher-dimensional cases

In the present section, we obtain upper bounds for the scaling of the time-asymptotic variance of the solutions of the system (2.1) along chosen functions  $g$ . In this case, we consider  $N > 1$ , therefore assuming that the system (2.1) is studied in higher spatial dimensions. We find that, for certain functions  $f : \mathcal{X} \subseteq \mathbb{R}^N \rightarrow \mathbb{R}$ , the early warning signs display convergence of the variance along the mentioned directions in the square-integrable function space,  $L^2(\mathcal{X})$ .

For the remainder of this section, we assume that  $f$  is analytic and satisfies (2.2) for  $x_* = 0 \in \mathcal{X} \subseteq \mathbb{R}^N$ . Hence,  $f$  is of the form

$$f(x) = - \sum_{j \in \mathcal{C}} a_j x^j \quad \text{for } x = (x_1, \dots, x_N) \in \mathcal{X}, \tag{4.1}$$

where  $j$  is a multi-index, i.e.,  $x^j = \prod_{n=1}^N x_n^{j_n}$  with the collection  $\mathcal{C}$  defined by the set

$$\mathcal{C} = \{j = (i_1, \dots, i_N) \in \{\mathbb{N} \cup \{0\}\}^N\}.$$

The coefficients  $a_j$  are real-valued, and their signs satisfy (2.2) as discussed further in the paper. We assume that there exists  $\varepsilon > 0$  such that  $[0, \varepsilon]^N \subseteq \mathcal{X}$ , up to rescaling of the space variable  $x$ . Properties (2.2) imply that equation (2.4) holds, hence for  $g(x) = \mathbb{1}_{[0,\varepsilon]^N}(x)$  we find

$$\langle g, V_\infty g \rangle = \sigma^2 \left\langle \frac{-1}{2(f+p)} g, g \right\rangle = \frac{\sigma^2}{2} \int_0^\varepsilon \dots \int_0^\varepsilon \frac{-1}{f(x) + p} dx = \frac{\sigma^2}{2} \int_0^\varepsilon \dots \int_0^\varepsilon \frac{1}{\sum_{j \in \mathcal{C}} a_j x^j - p} dx.$$

In the next proposition, we prove that for any  $f$  in a dense subset of the analytic functions space that satisfies (2.2), the variance  $\langle g, V_\infty g \rangle$  converges for  $p \rightarrow 0^-$ .

**Proposition 4.1.** Fix the dimension  $N > 1$ , and set the indices  $\{i_k\}_{k \in \{1, \dots, N\}}$  as a permutation of  $\{1, \dots, N\}$ . Furthermore, suppose that there exist two multi-indices  $j_1, j_2 \in \mathcal{C}$  such that  $a_{j_1}, a_{j_2} > 0$  and that each of these multi-indices corresponds to the multiplication of only one  $x_{i_1}$ , resp.  $x_{i_2}$ , meaning that  $j_1$ , resp.  $j_2$ , has all elements equal to 0 with the exception of the component on the  $i_1$ -th, resp.  $i_2$ -th, position which assumes value 1. Then it holds that

$$\lim_{p \rightarrow 0^-} \langle g, V_\infty g \rangle < \infty$$

for any  $\varepsilon > 0$  and  $g(x) = \mathbb{1}_{[0,\varepsilon]^N}(x)$ .

**Proof.** Without loss of generality, we assume that  $j_1 = (1, 0, 0 \dots)$  and  $j_2 = (0, 1, 0 \dots)$ . Then we obtain

$$\begin{aligned} \langle g, V_\infty g \rangle &= \frac{\sigma^2}{2} \int_0^\varepsilon \dots \int_0^\varepsilon \frac{1}{\sum_{j \in \mathcal{C}} a_j x^j - p} dx_N \dots dx_1 \\ &= \frac{\sigma^2}{2} \int_0^\varepsilon \dots \int_0^\varepsilon \frac{1}{a_{j_1} x_1 + a_{j_2} x_2 + \sum_{j \in \mathcal{C} \setminus \{j_1, j_2\}} a_j x^j - p} dx_N \dots dx_1 \\ &\leq C \frac{\sigma^2}{2} \int_0^\varepsilon \dots \int_0^\varepsilon \frac{1}{x_1 + x_2 - p} dx_N \dots dx_1 \end{aligned}$$

where the last inequality is satisfied by a constant  $C > 0$  and follows from the values  $a_{j_1}, a_{j_2} > 0 > p$ , the continuity of  $f$  and the compactness of the support of  $g$ . This implies that

$$\begin{aligned} \lim_{p \rightarrow 0^-} \int_0^\varepsilon \dots \int_0^\varepsilon \frac{1}{x_1 + x_2 - p} dx_N \dots dx_1 &= \varepsilon^{N-2} \lim_{p \rightarrow 0^-} \int_0^\varepsilon \int_0^\varepsilon \frac{1}{x_1 + x_2 - p} dx_2 dx_1 \\ &= \varepsilon^{N-2} \lim_{p \rightarrow 0^-} \int_0^\varepsilon \log(\varepsilon + x_1 - p) - \log(x_1 - p) dx_1 \\ &= \varepsilon^{N-2} \lim_{p \rightarrow 0^-} \left( (2\varepsilon - p) \log(2\varepsilon - p) - (2\varepsilon - p) - 2(\varepsilon - p) \log(\varepsilon - p) + 2(\varepsilon - p) - p \log(-p) + p \right) \\ &= \varepsilon^{N-2} \lim_{p \rightarrow 0^-} \left( (2\varepsilon - p) \log(2\varepsilon - p) - 2(\varepsilon - p) \log(\varepsilon - p) - p \log(-p) \right) < +\infty, \end{aligned}$$

which concludes the proof. □

**Example 4.2.** We study the trivial case in which we set  $f$  in (2.1) to be  $f_\infty(x) := 0$  for any  $x$  in a neighbourhood of  $x_*$ , in order to exclude it from the following computations. Whereas the function  $f_\infty$  does not satisfy the assumptions on the sign of  $f$  in (2.2), it provides an interesting and easy-to-study limit case. The time-asymptotic variance along the function  $g = \mathbb{1}_{[0,\varepsilon]^N}$  satisfies

$$\langle g, V_\infty g \rangle = \frac{\sigma^2}{2} \int_0^\varepsilon \dots \int_0^\varepsilon \frac{1}{f_\infty(x_1, \dots, x_N) - p} dx_N \dots dx_1 = \frac{\sigma^2}{2} \int_0^\varepsilon \dots \int_0^\varepsilon \frac{1}{-p} dx_N \dots dx_1 = -\frac{\sigma^2}{2p} \varepsilon^N.$$

Taking the limit in  $p$ , we obtain that

$$\lim_{p \rightarrow 0^-} \langle g, V_\infty g \rangle = \lim_{p \rightarrow 0^-} -\frac{\sigma^2}{2p} \varepsilon^N = \infty.$$

Hence, we observe divergence with rate  $\Theta(-p^{-1})$  for  $p$  approaching zero from below, if  $f$  in (2.1) is, locally, equal to the null function.

### 4.1 Upper bounds

In the remainder of this section, we find upper bounds for the scaling law of  $\langle g, V_\infty g \rangle$  for the case in which the dimension  $N$  of the domain of the function  $f$  is larger than 1. From the construction of  $f$  in (4.1), we define the set of multi-indices

$$\mathcal{C}^+ := \left\{ j = (i_1, \dots, i_N) \in \mathcal{C} \mid a_d = 0 \ \forall d = (d_1, \dots, d_N) \in \mathcal{C} \text{ s.t. } d_n \leq i_n \ \forall n \in \{1, \dots, N\} \text{ and } d \neq j \right\}. \tag{4.2}$$

The following lemma introduces an upper bound of  $\langle g, V_\infty g \rangle$  as  $p \rightarrow 0^-$ . The scaling law induced by this upper bound is studied further below.

**Lemma 4.3.** *Set  $f(x) = -\sum_{j \in C} a_j x^j$  for all  $x \in \mathcal{X} \subseteq \mathbb{R}^N$ , that satisfies (2.2),  $\{a_j\}_{j \in C} \subset \mathbb{R}$ ,  $\varepsilon > 0$  and  $Q = I$ . Fix  $j_* \in C^+$ , defined in (4.2). Then the time-asymptotic covariance of the solution of (2.1),  $V_\infty$ , satisfies,*

$$\langle g, V_\infty g \rangle \leq \Theta \left( \int_0^\varepsilon \cdots \int_0^\varepsilon \frac{1}{a_{j_*} x^{j_*} - p} dx_1 \dots dx_N \right),$$

for  $g(x) = \mathbb{1}_{[0, \varepsilon]^N}$ .

**Proof.** Since we assume  $f$  to be negative in  $\mathcal{X} \setminus \{0\}$  and we consider the bounded domain  $[0, \varepsilon]^N$ , we know that  $a_j > 0$  for any  $j \in C^+$ . In particular, we note that for a constant  $1 > C > 0$ , dependent on  $\varepsilon$ , and any  $x \in [0, \varepsilon]^N$ , it holds

$$-f(x) = \sum_{j \in C} a_j x^j \geq C \sum_{j \in C^+} a_j x^j \geq C a_{j_*} x^{j_*}$$

for  $j_* \in C^+$ . Hence, we obtain

$$\langle g, V_\infty g \rangle = \frac{\sigma^2}{2} \int_0^\varepsilon \cdots \int_0^\varepsilon \frac{1}{\sum_{j \in C} a_j x^j - p} dx_1 \dots dx_N \leq \frac{\sigma^2}{2C} \int_0^\varepsilon \cdots \int_0^\varepsilon \frac{1}{a_{j_*} x^{j_*} - p} dx_1 \dots dx_N. \quad (4.3)$$

Without loss of generality and for simplicity, we assume for the remainder of the section that  $a_{j_*} = \frac{\sigma^2}{2} = 1$ . □

**Remark 4.4.** *In case the multi-index  $j_*$  has  $N > k \in \mathbb{N} \cup \{0\}$  indices with value 0, the analysis on the upper bound in (4.3) can be reduced to the case of  $N - k$  spatial dimensions. In fact, assuming that  $j_* = (i_1, \dots, i_{N-k}, 0, \dots, 0)$ , we obtain*

$$\int_0^\varepsilon \cdots \int_0^\varepsilon \frac{1}{x^{j_*} - p} dx_1 \dots dx_N = \varepsilon^k \int_0^\varepsilon \cdots \int_0^\varepsilon \frac{1}{\prod_{n=1}^{N-k} x_n^{i_n} - p} dx_1 \dots dx_{N-k}.$$

We note that the case  $N = k$  contradicts the assumption  $f(x_*) = 0$  and results in convergence of the upper bound as the bifurcation threshold is not reached for  $p \rightarrow 0^-$ .

As a consequence of Remark 4.4, we consider  $j_*$  with no elements equal to 0 in the remaining subsections.

### 4.2 Two dimensions

In this subsection, we find an upper bound for the scaling law of  $\langle g, V_\infty g \rangle$  for  $N = 2$ . We therefore consider  $j_* = (i_1, i_2) \in \mathbb{N}^2$ . In the following theorem, we outline how to obtain such upper bounds.

**Theorem 4.5.** *Set  $f(x) = -\sum_{j \in C} a_j x^j$  for all  $x \in \mathcal{X} \subseteq \mathbb{R}^2$ , that satisfies (2.2),  $\{a_j\}_{j \in C} \subset \mathbb{R}$ ,  $\varepsilon > 0$  and  $Q = I$ .*

*Fix  $j_* = (i_1, i_2) \in C^+$  with  $i_1, i_2 > 0$ . Then there exists an upper bound to the time-asymptotic variance of the solution of (2.1) along  $g(x) = \mathbb{1}_{[0, \varepsilon]^2}$ ,  $\langle g, V_\infty g \rangle$ , and its rate as  $p \rightarrow 0^-$  is described in Table 3 in accordance to the value of  $i_1$  and  $i_2$ .*

The proof of the theorem can be found in Appendix A. Overall, we have obtained an upper bound for an analytic function  $f$ . In Table 3, we see that only the highest index  $i_2$  directly affects the scaling law of the upper bound. However, its relation to the other index  $i_1$  dictates the exact form. The limiting case for  $i_1, i_2 \rightarrow \infty$  has been discussed in Example 4.2. Lastly, we note that our bound may not be sharp, as described in Proposition 4.1 and as shown in the next example. Figure 2 presents an intuition for

**Table 3.** Upper bounds to the scaling law of the time-asymptotic variance in dimension  $N = 2$  for different choices of indices  $i_1, i_2$ , ordered for simplicity. We indicate as  $\mathfrak{A}$  and  $\mathfrak{B}$  two summands whose sum corresponds to the upper bound

Case	Scaling law for $p \rightarrow 0^-$		
	$\mathfrak{A}$	$\mathfrak{B}$	Upper bound
1: $i_2 > i_1 > 1$	$(-p)^{-1+\frac{1}{i_1}}$	$(-p)^{-1+\frac{1}{i_2}}$	$(-p)^{-1+\frac{1}{i_2}}$
2: $i_2 > i_1 = 1$	$-\log(-p)$	$(-p)^{-1+\frac{1}{i_2}}$	$(-p)^{-1+\frac{1}{i_2}}$
3: $i_2 = i_1 > 1$	$(-p)^{-1+\frac{1}{i_1}}$	$-(-p)^{-1+\frac{1}{i_2}} \log(-p)$	$-(-p)^{-1+\frac{1}{i_2}} \log(-p)$
4: $i_2 = i_1 = 1$	$-\log(-p)$	$\log^2(-p)$	$\log^2(-p)$

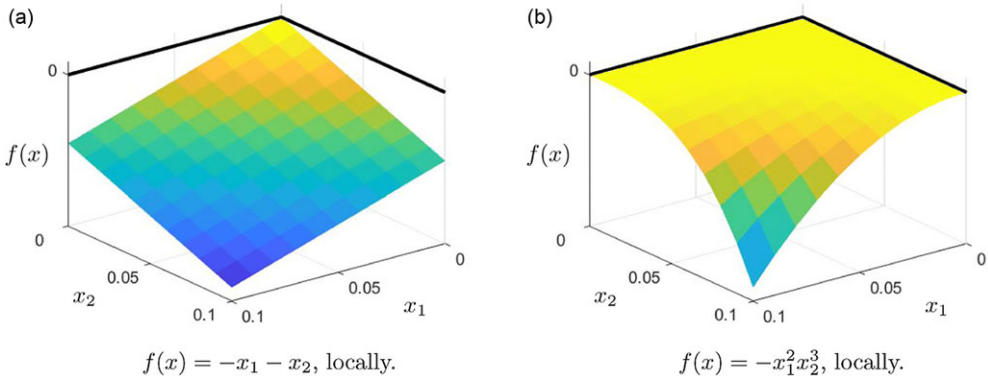


**Figure 2.** Illustration of functions  $-x_1 - x_2$ , in Figure a, and  $-x_1^2 x_2^3$ , in Figure b, for  $x_1, x_2 \in [0, 0.1]$ . We set an indicator function  $g = \mathbb{1}_{[0, \varepsilon]^2}$ , for  $0 < \varepsilon \leq 0.1$ . As discussed in Proposition 4.1 and in the proof of Theorem 4.5, the time-asymptotic variance  $\langle g, V_\infty g \rangle$  presents different scaling laws as  $p \rightarrow 0^-$  under distinct assumptions of  $f$ . For  $f$  set as in Figure a, the variance converges in the limit, whereas for  $f$  as displayed in Figure b, it diverges. We note that the choice of  $f$  in the Figure a presents only one value  $x_*$  such that  $f(x_*) = 0$ , in contrast with the second figure, for which  $f(x_1, x_2) = 0$  for any  $(x_1, x_2)$  such that  $x_1 = 0$  or  $x_2 = 0$ . Such lines are displayed in the figure for comparison.

the example  $j_* = (2, 3)$  by illustrating the shapes of  $-x_1 - x_2$  and  $-x_1^2 x_2^3$ , for  $(x_1, x_2) \in [0, 0.1]^2$ . Such functions can be assumed to be locally equal to  $f$  in Proposition 4.1 and Theorem 4.5, respectively. As displayed, the first function has a unique root on  $(0, 0)$ , and the second is null on the set  $(x_1, x_2)$  such that  $x_1 = 0$  or  $x_2 = 0$ . The different dimensions that characterise such sets are the reason for the fact that the time-asymptotic variance on an indicator function  $g$ ,  $\langle g, V_\infty g \rangle$ , presents different scaling laws in the limit  $p \rightarrow 0^-$ . In particular, it converges in the first case and diverges with rate  $(-p)^{-\frac{3}{2}}$  in the second.<sup>3</sup>

**Example 4.6.** We consider the function  $f$  such that it satisfies (2.2),  $[0, 1]^2 \subseteq \mathcal{X}$  and there exists  $C > 0$  for which

$$C^{-1} (-x_1^2 - x_2^2) \leq f(x) \leq C (-x_1^2 - x_2^2) ,$$

for  $0 \leq x_1, x_2 \leq 1$ . This implies that

$$\langle g, V_\infty g \rangle \leq C^{-1} \int_0^1 \int_0^1 \frac{1}{x_1^2 + x_2^2 - p} dx_1 dx_2 \leq C^{-1} \iint_D \frac{1}{x_1^2 + x_2^2 - p} dx_1 dx_2 \quad ,$$

<sup>3</sup>We underline that, although  $f(x) = -x_1^2 x_2^3$  in a neighbourhood of 0 does not satisfy (2.2), the scaling law of its time-asymptotic variance is proven in the proof of Theorem 4.5.

**Table 4.** Upper bounds to the scaling law of the time-asymptotic variance in dimension  $N = 3$  for different choices of indices  $i_1, i_2$  and  $i_3$ , ordered for simplicity. We denote as  $\mathfrak{C}$  and  $\mathfrak{D}$  two values whose sum is the upper bound

Case	Scaling law for $p \rightarrow 0^-$		
	$\mathfrak{C}$	$\mathfrak{D}$	Upper bound
1: $i_3 > i_2 > i_1 > 1$	$(-p)^{-1+\frac{1}{2}}$	$(-p)^{-1+\frac{1}{3}}$	$(-p)^{-1+\frac{1}{3}}$
2: $i_3 > i_2 = i_1 > 1$	$-(-p)^{-1+\frac{1}{2}} \log(-p)$	$(-p)^{-1+\frac{1}{3}}$	$(-p)^{-1+\frac{1}{3}}$
3: $i_3 = i_2 > i_1 > 1$	$(-p)^{-1+\frac{1}{2}}$	$-(-p)^{-1+\frac{1}{3}} \log(-p)$	$-(-p)^{-1+\frac{1}{3}} \log(-p)$
4: $i_3 = i_2 = i_1 > 1$	$-(-p)^{-1+\frac{1}{2}} \log(-p)$	$(-p)^{-1+\frac{1}{3}} \log^2(-p)$	$(-p)^{-1+\frac{1}{3}} \log^2(-p)$
5: $i_3 > i_2 > i_1 = 1$	$(-p)^{-1+\frac{1}{2}}$	$(-p)^{-1+\frac{1}{3}}$	$(-p)^{-1+\frac{1}{3}}$
6: $i_3 > i_2 = i_1 = 1$	$\log^2(-p)$	$(-p)^{-1+\frac{1}{3}}$	$(-p)^{-1+\frac{1}{3}}$
7: $i_3 = i_2 > i_1 = 1$	$(-p)^{-1+\frac{1}{2}}$	$-(-p)^{-1+\frac{1}{3}} \log(-p)$	$-(-p)^{-1+\frac{1}{3}} \log(-p)$
8: $i_3 = i_2 = i_1 = 1$	$\log^2(-p)$	$-\log^3(-p)$	$-\log^3(-p)$

where  $D$  denotes the circle of radius  $\sqrt{2}$  centred at the origin. We study then the integral in polar coordinates and obtain

$$\iint_D \frac{1}{x_1^2 + x_2^2 - p} dx_1 dx_2 = \int_0^{2\pi} \int_0^{\sqrt{2}} \frac{r}{r^2 - p} dr d\theta .$$

Substituting  $r' = r^2 - p$ , we get

$$\int_0^{2\pi} \int_0^{\sqrt{2}} \frac{r}{r^2 - p} dr d\theta = \frac{1}{2} \int_0^{2\pi} \int_{-p}^{2-p} \frac{1}{r'} dr' d\theta = \pi \left( \log(2 - p) - \log(-p) \right) = \Theta \left( -\log(-p) \right) .$$

A lower bound can be easily obtained through

$$\langle g, V_\infty g \rangle \geq C \int_0^1 \int_0^1 \frac{1}{x_1^2 + x_2^2 - p} dx_1 dx_2 \geq C \iint_D \frac{1}{x_1^2 + x_2^2 - p} dx_1 dx_2 = \Theta \left( -\log(-p) \right) ,$$

for  $\tilde{D} = \{(x, y) \mid x^2 + y^2 \leq 1, x, y > 0\}$ . Hence, we find divergence of  $\langle g, V_\infty g \rangle$ , for  $p$  approaching zero from below, of rate  $\Theta \left( -\log(-p) \right)$ , whereas the upper bounds in Theorem 4.5 assume scaling law  $\Theta \left( (-p)^{-\frac{1}{2}} \right)$ .

### 4.3 Three dimensions

We now assume  $N = 3$  and therefore  $f : \mathcal{X} \subseteq \mathbb{R}^3 \rightarrow \mathbb{R}$  and  $g = \mathbb{1}_{[0, \varepsilon]^3}$ . The following theorem provides an upper bound for the scaling law of the corresponding early warning sign  $\langle g, V_\infty g \rangle$ .

**Theorem 4.7.** Set  $f(x) = -\sum_{j \in \mathcal{C}} a_j x^j$  for all  $x \in \mathcal{X} \subseteq \mathbb{R}^3$  that satisfies (2.2),  $\{a_j\}_{j \in \mathcal{C}} \subset \mathbb{R}$ ,  $\varepsilon > 0$  and  $Q = I$ . Fix  $j_* = (i_1, i_2, i_3) \in \mathcal{C}^+$  with  $i_1, i_2, i_3 > 0$ . Then there exists an upper bound to the time-asymptotic variance of the solution of (2.1) along  $g(x) = \mathbb{1}_{[0, \varepsilon]^3}$ ,  $\langle g, V_\infty g \rangle$ , and it has a scaling law bound as  $p \rightarrow 0^-$  described in Table 4 depending upon the values of  $i_1, i_2$  and  $i_3$ .

The theorem is proven in Appendix B. We observe that if  $i_3$  is strictly greater than the other indices,  $i_1$  and  $i_2$ , we find divergence with the upper bound  $\Theta \left( (-p)^{-1+\frac{1}{3}} \right)$ . If the highest index value is given by two of the indices, i.e.,  $i_3 = i_2 > i_1$ , then the upper bound to the scaling is  $\Theta \left( -(-p)^{-1+\frac{1}{3}} \log(-p) \right)$ . We see also that in the case all three indices are equal but greater than 1, i.e.,  $i_3 = i_2 = i_1 > 1$ , then the upper

bound is  $\Theta \left( (-p)^{-1+\frac{1}{5}} \log^2(-p) \right)$ . Lastly, setting all the indices equal to 1, the corresponding rate is  $\Theta \left( -\log^3(-p) \right)$ . In Example 4.2, the limit case  $i_1, i_2, i_3 \rightarrow \infty$  is covered.

## 5 Generalisations and examples

### 5.1 Generalisations

We now generalise and discuss the main results obtained above, focusing on the impact of relaxing the hypotheses in Section 2. In particular, similar results to those presented in Theorems 3.3, 4.5 and 4.7 can be obtained under slightly more general choices of functions  $f, g$  and operator  $Q$ . We also study the theorems for  $T_f$  with complex spectrum. Lastly, we discuss the case in which different linear operators,  $A$ , with continuous spectrum are presented in the drift term of (2.1).

► The condition of the uniqueness of  $x_*$  such that  $f(x_*) = 0$  is required only in a local sense. In fact, we could assume the existence of  $\mathcal{Z} \subset \mathcal{X}$  for which any  $x \in \mathcal{Z}$  satisfies  $f(x) = 0$  and  $\text{dist}(x_*, x) > 0$ . Such a choice would trivially leave unchanged the scaling laws described in Theorems 3.3, 4.5 and 4.7, for functions  $g$  such that the support of  $g$  has an empty intersection with  $\mathcal{Z}$ . The analytic behaviour of the non-positive function  $f$  presented in Theorems 3.3, 4.5 and 4.7 can be assumed only in a neighbourhood of the roots of the function, while  $f$  satisfies the integrability condition in (2.2) and the sign properties previously described.

► In Theorems 3.3, 4.5 and 4.7, the support of the function  $g$  is assumed to be  $[0, \varepsilon]^N$  and  $g$  to be an indicator function, yet the scaling laws in Tables 1, 3 and 4 are applicable for a more general choice. First, similarly to Remark 3.5, the upper bounds described in Theorems 4.5 and 4.7 can be shown to hold with  $g = \mathbb{1}_{[-\varepsilon, \varepsilon]^N}$ , in the sense that the hypercube  $[-\varepsilon, \varepsilon]^N \subseteq \mathcal{X}$  that describes the support of  $g$  can be split in  $2^N$  hypercubes on which such statements have been proven, up to reparametrisation and rescaling of the spatial variable  $x$ , and of which only the highest rate of divergence dictates the order assumed by the upper bound of  $\langle g, V_\infty g \rangle$ . The shape of the support can also be generalised. Set  $g = \mathbb{1}_S$  for  $[-\varepsilon, \varepsilon]^N \subseteq S \subseteq \mathcal{X}$ , then the integral

$$\langle g, V_\infty g \rangle = \frac{\sigma^2}{2} \int_S \frac{-1}{f(x) + p} dx = \frac{\sigma^2}{2} \int_{S \setminus [-\varepsilon, \varepsilon]^N} \frac{-1}{f(x) + p} dx + \frac{\sigma^2}{2} \int_{[-\varepsilon, \varepsilon]^N} \frac{-1}{f(x) + p} dx$$

assumes an equivalent rate of divergence to the second summand on the right-hand side of the equation. That is implied by the fact that the first summand converges as  $p \rightarrow 0^-$  by construction. The scaling law is also unchanged under the assumption of  $g \in L^2(\mathcal{X})$  such that  $g$  and  $g^{-1}$  are bounded from above in a neighbourhood of  $x_*$  as, for any  $p < 0$ , it holds

$$C^{-1} \frac{\sigma^2}{2} \int_S \frac{-1}{f(x) + p} dx \leq \langle g, V_\infty g \rangle \leq C \frac{\sigma^2}{2} \int_S \frac{-1}{f(x) + p} dx,$$

for a constant  $C > 1$  depending on  $g$  and on the choice of  $S$ . Lastly, assume  $g_1, g_2 \in L^2(\mathcal{X})$  which are continuous in a neighbourhood  $\mathcal{S}$  of  $x_*$  and such that  $g_1, g_2, g_1^{-1}$  and  $g_2^{-1}$  are bounded from above in  $\mathcal{S}$ . We note that such a set of functions is dense in  $L^2(\mathcal{X})$ . For simplicity, we set  $g_1(x_*)g_2(x_*) > 0$ . The scaling law of the scalar product in (2.4) can be obtained through

$$C^{-1} \frac{\sigma^2}{2} \int_S \frac{-1}{f(x) + p} dx \leq \langle g_1, V_\infty g_2 \rangle \leq C \frac{\sigma^2}{2} \int_S \frac{-1}{f(x) + p} dx,$$

for  $C > 1$  and any  $p$  close to 0, thus enabling a study of the covariance operator  $V_\infty$ .

► A third generalisation of Theorems 3.3, 4.5 and 4.7 is given by relaxing the assumptions for  $Q$ . We can assume  $Q$  and its inverse on  $L^2(\mathcal{X})$ ,  $Q^{-1}$ , to have bounded eigenvalues from above. The covariance operator ([16, Theorem 5.2]) takes the form

$$V_\infty = \sigma^2 \int_0^\infty e^{\tau(T_f + p)} Q e^{\tau(T_f + p)} d\tau.$$

Hence, we get

$$\langle g, V_\infty g \rangle = \sigma^2 \int_0^\infty \langle \sqrt{Q} e^{t(T_f+p)} g, \sqrt{Q} e^{t(T_f+p)} g \rangle dt = \sigma^2 \int_0^\infty \|\sqrt{Q} e^{t(T_f+p)} g\|^2 dt,$$

for any  $g \in L^2(\mathcal{X})$ . Since we have assumed that  $Q$  and its inverse have bounded eigenvalues from above, the scalar product is also bounded from below and above, as we have

$$\inf_n q_n \sigma^2 \int_0^\infty \|e^{(T_f+p)t} g\|^2 dt \leq \sigma^2 \int_0^\infty \|\sqrt{Q} e^{(T_f+p)t} g\|^2 dt \leq \sup_n q_n \sigma^2 \int_0^\infty \|e^{(T_f+p)t} g\|^2 dt, \tag{5.1}$$

with  $\{q_n\}_{n \in \mathbb{N}}$  referring to the eigenvalues of  $Q$ . This implies that we have found an upper and lower bound for  $\langle g, V_\infty g \rangle$  whose scaling law is controlled in accordance with the results in Theorems 3.3, 4.5 and 4.7. Therefore, the rate of divergence for the choices of  $f$  and  $g$  described in the theorems or in the previous generalisations is displayed in Tables 1, 3 and 4, in accordance to the value of dimension  $N \in \{1, 2, 3\}$ . Assuming instead  $Q$  to be bounded, the validity of the rates of the upper bound in Theorems 4.5 and 4.7 is maintained as the second inequality in (5.1) holds.

► We now consider the case in which the spectrum of  $A = T_f$  has complex values, i.e., we choose a function  $f : \mathcal{X} \subseteq \mathbb{R}^N \rightarrow \mathbb{C}$  and the solution of (2.1) as  $u \in L^2(\mathcal{X}; \mathbb{C})$ . We suppose also that  $\text{Re}(f)$  satisfies (2.2). The scalar product of the covariance operator takes then the form

$$\langle g, V_\infty g \rangle = \int_{\mathcal{X}} \overline{g(x)} \int_0^\infty e^{\overline{f(x)+p)t} e^{f(x)+p)t} g(x) dt dx = - \int_{\mathcal{X}} |g(x)|^2 \frac{\sigma^2}{2(\text{Re}(f(x)) + p)} dx.$$

for any  $g \in L^2(\mathcal{X}; \mathbb{C})$ . Assuming that  $\text{Re}(f(x))$  is analytic, we conclude that the rate of divergence, or its upper bound if  $N > 1$ , of the studied time-asymptotic variance along almost any  $g \in L^2(\mathcal{X}; \mathbb{C})$  behaves equivalently to those indicated by Theorems 3.3, 4.5 and 4.7 under the choices of real-valued functions  $\text{Re}(f(x))$ , associated to the multiplication operator, and  $|g(x)|$ , as the direction along which the corresponding time-asymptotic variance is studied.

► Lastly, we study the system

$$\begin{cases} du(x, t) = (A + p) u(x, t) dt + \sigma dW(t) \\ u(\cdot, 0) = u_0 \end{cases} \tag{5.2}$$

for  $A$  a linear self-adjoint operator in  $L^2(\mathcal{X})$  with non-positive spectrum. The spectral theorem [25, Theorem 10.10] implies the existence of a  $\sigma$ -finite measure space  $(\mathcal{X}_0, \mu)$ , a measurable function  $\tilde{f} : \mathcal{X}_0 \rightarrow \mathbb{R}$  and a unitary map  $U : L^2(\mathcal{X}) \rightarrow L^2(\mathcal{X}_0, \mu)$  such that

$$U(L^2(\mathcal{X})) = \left\{ \tilde{g} \in L^2(\mathcal{X}_0, \mu) \mid \tilde{f} \tilde{g} \in L^2(\mathcal{X}_0, \mu) \right\}$$

and

$$UAU^{-1} = T_{\tilde{f}},$$

for  $T_{\tilde{f}} : L^2(\mathcal{X}_0, \mu) \rightarrow L^2(\mathcal{X}_0, \mu)$  a multiplication operator for  $\tilde{f}$ . Assuming  $e^{A+p}$  to have finite trace, the time-asymptotic covariance operator for the solution of (5.2) is

$$\langle g, V_\infty g \rangle = \sigma^2 \int_0^\infty \langle e^{2t(A+p)} g, g \rangle dt,$$

for  $Q = I$  and  $g \in L^2(\mathcal{X})$ . Labelling  $\tilde{g} = Ug$  we obtain through Fubini's Theorem that

$$\begin{aligned} \langle g, V_\infty g \rangle &= \sigma^2 \int_0^\infty \langle U^{-1} e^{2t(T_f+p)} Ug, g \rangle dt = \sigma^2 \int_0^\infty \langle e^{2t(T_{\tilde{f}}+p)} \tilde{g}, \tilde{g} \rangle_{L^2(\mathcal{X}_0, \mu)} dt \\ &= \int_{\mathcal{X}_0} \tilde{g}(x) \int_0^\infty e^{2\tilde{f}(x)+2p)t} \tilde{g}(x) dt d\mu(x) = - \int_{\mathcal{X}_0} \tilde{g}(x)^2 \frac{\sigma^2}{2(\tilde{f}(x) + p)} d\mu(x). \end{aligned}$$

The operators  $A$  and  $T_{\tilde{f}}$  have the same spectrum. We can assume that there exists an interval  $(-\delta, 0]$  in the continuous spectrum of  $A$ , which yields that  $\mu(\{\tilde{f} = 0\}) = 0$  and that there exists at least a

point  $x_* \in \mathcal{X}_0$  such that  $\tilde{f}(x_*) = 0$ . From the Stone–Weierstrass theorem, we know that, for  $g$  in a dense subset of  $L^2(\mathcal{X})$ , the associated  $\tilde{g} \in L^2(\mathcal{X}_0, \mu)$  assumes bounded and non-null values  $\mu$ -a.e. in a neighbourhood of each root  $x_*$ . The scaling law for the case  $N = 1$  can be studied similarly to Remark 3.4, given insights about the measure  $\mu$  and assuming  $\tilde{f}$  analytic ([25]). Such an assumption is not restrictive for  $A$  bounded since such a condition implies that  $\tilde{f}$  is bounded [25, Theorem 7.20]. In fact, we fix  $x_*$ , a neighbourhood  $\mathcal{X}_1 \subseteq \mathcal{X}_0$  and define

$$\begin{aligned} S_p &= \{ \tilde{f} : \mathcal{X}_1 \rightarrow \mathbb{R} \mid \tilde{f} \text{ is polynomial, } \tilde{f}(x_*) = 0 \}, \\ S_a &= \{ \tilde{f} : \mathcal{X}_1 \rightarrow \mathbb{R} \mid \tilde{f} \text{ is analytic, } \tilde{f}(x_*) = 0 \}, \\ S_c &= \{ \tilde{f} : \mathcal{X}_1 \rightarrow \mathbb{R} \mid \tilde{f} \text{ is continuous, } \tilde{f}(x_*) = 0 \}, \\ S_b &= \{ \tilde{f} : \mathcal{X}_1 \rightarrow \mathbb{R} \mid \tilde{f} \text{ is bounded, } \tilde{f}(x_*) = 0 \}, \\ S_l &= \{ \tilde{f} : \mathcal{X}_1 \rightarrow \mathbb{R} \mid \tilde{f} \in L^2(\mathcal{X}_1), \tilde{f}(x_*) = 0 \}. \end{aligned}$$

Stone–Weierstrass Theorem states that  $S_p$ , and thus  $S_a$ , is dense in  $S_c$ . Also,  $S_c$  is dense in  $S_l$ , and therefore in  $S_b$ . Hence, elements in  $S_a \cap \{ \tilde{f} : \mathcal{X}_1 \rightarrow \mathbb{R} \mid \tilde{f}(x) < 0 \text{ for } x \neq x_* \}$  can approximate functions in  $S_b \cap \{ \tilde{f} : \mathcal{X}_1 \rightarrow \mathbb{R} \mid \tilde{f}(x) < 0 \text{ for } x \neq x_* \}$ . Such sets of functions can be treated due to [25, Proposition 7.21].

### 5.2 Examples

In the current subsection, we provide general examples for the previously introduced generalisations. The focus is on different operators observed in Fourier space. Such a choice is also justified by their significance in applications, in particular for the widely studied differential operators [7, 57]. Specific systems relevant to modelling real-life phenomena are described in Section 7.

**Example 5.1.** Fix a non-positive function  $f : \mathbb{R} \rightarrow \mathbb{R}$  that satisfies (2.2). Consider the linear operator  $A : \mathcal{D}(A) \rightarrow L^2(\mathbb{R})$  such that for any  $g \in \mathcal{D}(A)$  it holds

$$Ag(x) = f * g(x) \quad , \quad \mathcal{D}(A) := \left\{ g \text{ Lebesgue measurable} \mid f * g \in L^2(\mathcal{X}) \right\} \quad ,$$

where  $*$  denotes convolution. We want to study the variance of the solution of the system (5.2) for  $Q$  bounded with bounded inverse and  $u_0 \in \mathcal{D}(A)$ . We define the Fourier transform  $\mathcal{F} : L^2(\mathbb{R}) \rightarrow L^2(\mathbb{R})$ , which is a unitary map. Assume  $g \in L^2(\mathbb{R})$ , then

$$\begin{aligned} \langle g, V_\infty g \rangle &= \sigma^2 \int_0^\infty \langle e^{t(A+p)} Q e^{t(A+p)} g, g \rangle dt = \sigma^2 \int_0^\infty \| \sqrt{Q} e^{t(A+p)} g \|^2 dt = \Theta \left( \int_0^\infty \| e^{t(A+p)} g \|^2 dt \right) \\ &= \Theta \left( \int_0^\infty \| \mathcal{F}^{-1} e^{t(T_f+p)} \mathcal{F} g \|^2 dt \right) = \Theta \left( \int_0^\infty \| e^{t(T_f+p)} \mathcal{F} g \|^2 dt \right). \end{aligned}$$

The scaling law of the variance can thus be computed, or compared, through Theorem 3.1 for  $f$  that satisfies (3.2) for  $\alpha > 0$  and for  $g$  in a dense subset of  $L^2(\mathbb{R})$ . As an example, we consider

$$f = \begin{cases} -|x| & , \quad \text{for } x \in [-1, 1] \\ -x^2 & , \quad \text{for } x \in \mathbb{R} \setminus [-1, 1] \end{cases}$$

and  $g = \mathcal{F}^{-1} \mathbb{1}_{[-\varepsilon, \varepsilon]}$ . The rate of divergence of the time-asymptotic variance is therefore  $-\log(-p)$  as  $p \rightarrow 0^-$ .

**Example 5.2.** Consider the self-adjoint operator  $A : \mathcal{H}^{2m}(\mathbb{R}) \rightarrow L^2(\mathbb{R})$  for  $m \in \mathbb{N}$  such that

$$Ag(x) = (-1)^{(m-1)} \partial_x^{2m} g(x) ,$$

where  $\partial_x$  denotes the weak derivative on  $\mathcal{H}^1(\mathbb{R})$ , and assume  $g \in \mathcal{H}^{2m}(\mathbb{R})$ . We want to study the variance of the solution of (5.2) for  $u_0 \in \mathcal{H}^{2m}(\mathbb{R})$ ,  $p < 0$  and  $Q$  a bounded operator with bounded inverse.



For  $g \in \mathcal{H}^{2m}(\mathbb{R})$  and  $f(k) = -k^{2m}$  for any  $k \in \mathbb{R}$ , we find that

$$\begin{aligned} \langle g, V_\infty g \rangle &= \sigma^2 \int_0^\infty \langle e^{t(A+p)} Q e^{t(A+p)} g, g \rangle dt = \Theta \left( \int_0^\infty \|e^{t(A+p)} g\|^2 dt \right) \\ &= \Theta \left( \int_0^\infty \|\mathcal{F}^{-1} e^{t(T_f+p)} \mathcal{F} g\|^2 dt \right) = \Theta \left( \int_0^\infty \|e^{t(T_f+p)} \mathcal{F} g\|^2 dt \right). \end{aligned}$$

From Theorem 3.1, the scaling law as  $p \rightarrow 0^-$  for  $g$  in a dense subset of  $\mathcal{H}^{2m}(\mathbb{R})$  is therefore  $\Theta \left( p^{-1+\frac{1}{2m}} \right)$ .

**Example 5.3.** We introduce the self-adjoint operator  $A(p) : \mathcal{H}^2(\mathbb{R}) \rightarrow L^2(\mathbb{R})$  such that  $A(p)$  has negative spectrum for  $p < 0$ . We assume the existence and uniqueness of  $\lambda(p)$ , an isolated element in its spectrum that satisfies  $\lambda(0) = 0$  and is continuous in  $p$ . The spectrum is assumed to be purely absolutely continuous for any  $p \leq 0$  and supported in  $(-\infty, \lambda(p)]$ . The mentioned assumptions are satisfied, for instance, by certain Schrödinger operators  $A(p) = \Delta - v(p, \cdot)$  for a bounded real potential  $v(p, \cdot)$  with compact support for any  $p \leq 0$  [18]. For any  $g \in L^2(\mathcal{X})$ ,  $p \leq 0$  and any continuous function  $f$ , we define the absolutely continuous measure with respect to the Lebesgue measure  $\mu_{g,p}$ , such that

$$\langle g, f(A(p))g \rangle = \int_{-\infty}^{\lambda(p)} f(x) d\mu_{g,p}(x).$$

It follows that the time-asymptotic covariance operator associated with the solutions of

$$\begin{cases} du(x, t) = A(p) u(x, t) dt + \sigma dW(t) \\ u(\cdot, 0) = u_0 \end{cases}$$

and  $Q = I$  satisfies

$$\langle g, V_\infty g \rangle = \sigma^2 \int_{-\infty}^{\lambda(p)} \int_0^\infty e^{2tx} dt d\mu_{g,p}(x) = -\frac{\sigma^2}{2} \int_{-\infty}^{\lambda(p)} \frac{1}{x} d\mu_{g,p}(x),$$

for any  $p < 0$ . We introduce the Radon–Nikodym derivative  $r_{g,p}(x) = \frac{d\mu_{g,p}(x)}{dx}$ . Under the assumption of continuity of  $r_{g,p}$  on  $p$ , we obtain that

$$\langle g, V_\infty g \rangle = -\frac{\sigma^2}{2} \int_{-\infty}^{\lambda(p)} \frac{r_{g,p}(x)}{x} dx$$

and the scaling law of the early warning sign.

**Remark 5.4.** The early warning sign in the form of the divergence of the time-asymptotic variance of the solution of a linearised system (5.2) has been studied in the case of the linear non-positive self-adjoint operator  $A$  with discrete spectrum [5, 24, 43]. An example to such an operator is  $\partial_x^2 : \mathcal{H}^2([-L, L]) \rightarrow L^2([-L, L])$  with Neumann boundary conditions. Its eigenvalues are known to be  $\{-\lambda_i\}_{i \in \mathbb{N}}$  for  $\lambda_i = \left(\frac{i\pi}{L}\right)^2$  and corresponding eigenfunctions  $e_i(\cdot) := \cos(\lambda_i \cdot)$ . For  $g \in \mathcal{H}^2([-L, L])$ , the time-asymptotic variance of the solution of (5.2) is

$$\langle g, V_\infty g \rangle = \frac{\sigma^2}{2} \sum_{i \in \mathbb{N}} \frac{\langle g, e_i \rangle^2}{\lambda_i - p}, \tag{5.3}$$

which is proven in [5]. Under the assumption that the projection of  $g$  along the most sensible eigenfunction  $e_i$  is not zero,  $\langle g, e_i \rangle \neq 0$ , the rate of divergence of the variance is of order  $\Theta \left( (-p)^{-1} \right)$  as  $p \rightarrow 0^-$ , similar to the case  $\alpha \rightarrow \infty$  in Table 1.

In the limit  $L \rightarrow \infty$ , the spectrum of the operator  $\partial_x^2 : \mathcal{H}^2(\mathbb{R}) \rightarrow L^2(\mathbb{R})$  is continuous and the rate of the divergence of time-asymptotic variance of the solution of the linearised system (5.2) can be obtained

as described in Example 5.2. In detail,

$$\begin{aligned} \langle g, V_\infty g \rangle &= \sigma^2 \int_0^\infty \langle e^{t2(\partial_x^2+p)} g, g \rangle dt = \sigma^2 \int_0^\infty \langle \mathcal{F}^{-1} e^{t2(\partial_x^2+p)} \mathcal{F}g, g \rangle dt \\ &= \sigma^2 \int_0^\infty \int_{\mathbb{R}} e^{2t(-k^2+p)} \mathcal{F}g(k)^2 dk dt = \frac{\sigma^2}{2} \int_{\mathbb{R}} \frac{\mathcal{F}g(k)^2}{k^2 - p} dk. \end{aligned} \tag{5.4}$$

We define the functions  $d_k(x) = e^{-2\pi i k x}$  for  $x, k \in \mathbb{R}$  and the imaginary unit  $i$ . Under the assumption that  $\mathcal{F}g$  assumes bounded non-zero values in a neighbourhood of  $k = 0$ , i.e., the projections of function  $g$  along the most sensible functions in  $\{d_k\}_{k \in \mathbb{R}}$  are bounded and non-zero, the rate of divergence of such variance is of order  $\Theta\left((-p)^{-\frac{1}{2}}\right)$  as proven in Example 5.2.

Intuitively, the difference of the rates of (5.3) and (5.4) is implied by the different shape of the spectrum of  $\partial_x^2$  for the finite or infinite value of  $L$ . In particular, as  $p$  crosses 0 from below in the case  $L < \infty$ , the solution of (5.2) is repelled by the linear term along  $e_0$ . Conversely, for  $p \rightarrow 0^-$  in the case  $L = \infty$ , the most unstable direction  $d_0$ , the constant function, is not in the domain of the operator.

### 6 Numerical simulations

In this section, we numerically investigate the analytic results from Sections 3 and 4 to gain more insight and also to obtain an outlook on how they can be relevant in a more applied setting. The numerical methods used and discussed follow the theory of [28] and [47].

We start by simulating a generalisation of the results obtained in Theorem 3.1 for the one-dimensional case and the tool function  $f_\alpha(x) = -|x|^\alpha$  on an interval for  $\alpha > 0$ . In order to approximate the solution of the studied SPDE, we use the Euler–Maruyama method, which we introduce considering the differential equation

$$du(x, t) = (f_\alpha(x) + p) u(x, t) dt + \sigma dW(t), \quad u(\cdot, 0) = u_0, \quad 0 \leq t \leq T, \tag{6.1}$$

for  $\sigma, T > 0 > p$ , initial condition  $u_0 \in L^2(\mathcal{X})$  and (boundary) conditions  $f_\alpha u \in L^2(\mathcal{X})$ . We then discretise the time interval  $[0, T]$  by defining the time step  $\delta t = \frac{T}{n\tau}$  for a certain positive integer  $n\tau$ , to be the number of steps in time, and  $\tau_i := i \delta t$ , the time passed after  $i$  time steps. Further, we discretise also the space interval  $\mathcal{X} = [-L, L]$  into its internal points  $r_n = -L + 2 \frac{n}{N+1} L$  for  $n \in \{1, \dots, N\}$ , with  $N$  being an integer that defines the number of mesh points. The numerical approximations of  $u(\cdot, \tau_i)$ ,  $f_\alpha$  and  $W(\cdot, \tau_i)$  are labelled, respectively as  $u_i, f_\alpha, W_i \in \mathbb{R}^{N+2}$  for any  $i \in \{0, \dots, n\tau\}$ . Then, by the implicit Euler–Maruyama method, the numerical simulation takes the form

$$u_i = u_{i-1} + (f_\alpha + p)u_i \delta t + \sigma(W_i - W_{i-1}), \quad i = 1, 2, \dots, n\tau$$

which approximates the integral form of the SPDE. For fixed  $i \in \{1, \dots, n\tau\}$ , the term  $W_i - W_{i-1}$  can be expressed as

$$W_i - W_{i-1} = \sqrt{\delta t} \sum_{m=1}^M \sqrt{q_m} W_i^{(m)} \mathbf{b}_m$$

with  $M \leq N$  being the number of directions in the space function on which the noise is taken numerically into account,  $\{W_i^{(m)}\}_{m \in \{1, \dots, M\}}$  a collection of independent standard Gaussian random variables and the randomly generated  $\{(q_m, \mathbf{b}_m)\}_{m \in \{1, \dots, M\}}$ , which are, respectively, the first  $M$  eigenvalues and approximations in  $\mathbb{R}^{N+2}$  of the eigenfunctions of the covariance operator  $Q$  of  $W$  in (6.1).<sup>4</sup>

We numerically simulate a generalisation of results from Theorem 3.1, as described in Section 5, for the function  $f_\alpha = -|x|^\alpha$  for  $\alpha > 0$  as defined by (3.1). We consider the case  $g(x) = \mathbb{1}_{[-\varepsilon, \varepsilon]}$  for

<sup>4</sup>The eigenvalues  $\{(q_m)\}_{m \in \{1, \dots, M\}}$  are generated uniformly in  $[0.5, 2]$ .

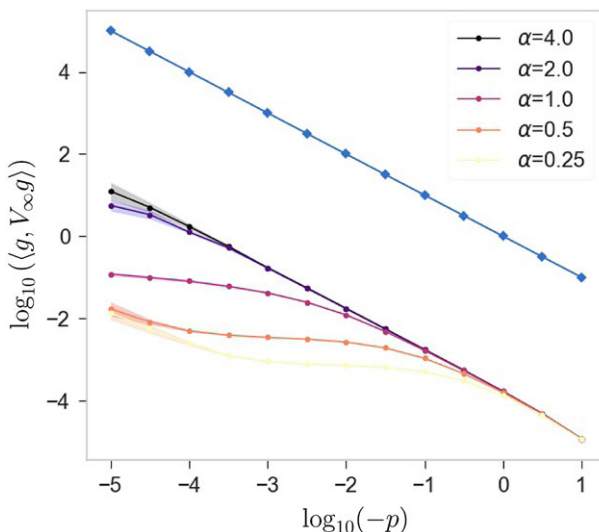


**Figure 3.** Log-log plot that describes the behaviour of  $\langle g, V_\infty g \rangle$  as  $p$  approaches  $0^-$  in accordance to the choice of the tool function  $f_\alpha$ . The circles are obtained as the mean value of  $\log_{10}(\langle g, V_\infty g \rangle)$  given by 10 independent simulations. The shaded areas have a width equal to the numerical standard deviation. Lastly, the blue line has a slope equal to  $-1$  and is provided as a reference for the scaling law. For  $\alpha \geq 1$ , the expected slope from Theorem 3.1 is shown close to  $p = 10^{-5}$ . The convergence is visible for  $\alpha < 1$  until  $p$  assumes small values. In fact, for small  $N$ , the log-log plot displays slope  $-1$  induced by the divergence being only perceived on  $x = 0$  and therefore leading to a behaviour similar to that of an OrnsteinUhlenbeck process [41].

$\{|r_n \in [-\varepsilon, \varepsilon] \mid n \in \{1, \dots, N\}\}| = M$ .<sup>5</sup> Further, we assume  $Q$  and its inverse  $Q^{-1}$  to be bounded operators. The fact that  $Q$  is not assumed to be the identity operator makes the random variables  $u(x_1, t)$  and  $u(x_2, t)$  dependent for any  $x_1, x_2 \in \mathcal{X}$  and  $t > 0$ . Hence, the simulation of  $u$  must be studied as an SPDE rather than a collection of SDEs on the resolution points. As described in Section 5, such a choice of  $Q$  is expected to imply scaling laws, dependent on  $\alpha$ , of the time-asymptotic variance as displayed in Table 1.

We simulate the projection  $\langle u(\cdot, \tau_i), g \rangle$  with  $\text{proj}_i = \sum_{n:r_n \in [-\varepsilon, \varepsilon]} u_i(n)$  for any  $i \in \{1, \dots, nt\}$ . We approximate the behaviour of the scalar product that defines the variance along  $g$ ,  $\langle g, V_\infty g \rangle$ , as the numerical variance in time  $i$  of  $\text{proj}_i$ . The results are displayed as a log-log plot in Figure 3. As we are interested in the behaviour for  $p$  approaching zero from below, we focus on negative values of  $\log_{10}(-p)$ . Validating the analytic results in Table 1, for  $\alpha > 1$  we observe  $\log_{10}(\langle g, V_\infty g \rangle)$  to assume a negative slope of  $-1 + \frac{1}{\alpha}$  as  $\log_{10}(-p)$  approaches  $-\infty$ . In the case  $\alpha = 1$ , we expect a logarithmic divergence in the log-log plot as  $\log_{10}(-p)$  decreases. Lastly, we expect convergence for  $0 < \alpha < 1$ , which is shown up to small values of  $p$  due to numerical errors.<sup>6</sup>

Next, we study the two-dimensional case and numerically simulate the asymptotic behaviour of the upper bound of  $\langle g, V_\infty g \rangle$  as described in Theorem 4.5. In particular, our goal is to illustrate the results analytically found for indices  $i_1, i_2$  such that  $i_2 \geq i_1 \geq 1$ . For this case, we have found the scaling law of

<sup>5</sup>The orthogonal matrix whose indices are  $\{b_m(n) \mid r_n \in [-\varepsilon, \varepsilon]\}_{m \in \{1, \dots, M\}}$  is generated through  $O(M)$  Haar distribution, for  $O(M)$  that indicates the space of orthogonal  $M \times M$  matrices with real-valued elements [51]. The rest of the elements in  $\{(b_m)\}_{m \in \{1, \dots, M\}}$ , which are irrelevant to the study of the time-asymptotic variance along  $g$ , can be obtained through Gram-Schmidt method.

<sup>6</sup> $L = 1, N = 99999, nt = 10000000, \delta t = 0.1, \sigma = 0.01, \varepsilon = 0.01, M = 999$ .

the upper bound as displayed in Table 3. We therefore compute the dependence of  $\int_0^\varepsilon \int_0^\varepsilon \frac{1}{x_1^{i_1} x_2^{i_2} - p} dx_1 dx_2$  on  $p < 0$  in a log-log plot.

The subfigures shown in Figure 4 are obtained for different choices of  $\varepsilon$  and of  $i_2 \geq i_1 \geq 1$ . We see that the results are confirmed as the double integrals, displayed as solid lines, show a similar qualitative behaviour as the analytic result in Table 3, corresponding to the red circles, for small values of  $-p$ . In particular, in the Figure 4a, b, c and d, corresponding to Case 1 and Case 2 of the table, we obtain a slope equal to  $-1 + \frac{1}{i_2}$ . The red circles in Figure 4e and f, corresponding to Case 3, have values

$$\log_{10}(-p) \left(-1 + \frac{1}{i_2}\right) + \log_{10}(-\log_{10}(-p)) + c$$

and the values in Figure 4g and h, corresponding to Case 4, are equal to

$$2\log_{10}(-\log_{10}(-p)) + c,$$

for different constants  $c$ . Decreasing the parameter  $\varepsilon > 0$  appears to imply a decrease of the lowest threshold  $q_c > 0$  such that for any  $-p > q_c$  the slope of  $\log_{10}\left(\int_0^\varepsilon \int_0^\varepsilon \frac{1}{x_1^{i_1} x_2^{i_2} - p} dx_1 dx_2\right)$  in the log-log plot is approximately  $-1$ . Such a slope is implied by the fact that, for  $p \ll 0$ , the values of  $x_1^{i_1} x_2^{i_2} - p$  present the same order of distance from 0 for any  $x_1, x_2 \in [0, \varepsilon]$  and, therefore, the early warning sign displays similar behaviour to those discussed in [5, 24, 43] for such values of  $p$ .

Lastly, we illustrate the results of Theorem 4.7 by computing the values of  $\int_0^\varepsilon \int_0^\varepsilon \int_0^\varepsilon \frac{1}{x_1^{i_1} x_2^{i_2} x_3^{i_3} - p} dx_1 dx_2 dx_3$  on  $p < 0$  in a log-log plot for different values of  $i_3 \geq i_2 \geq i_1 \geq 1$ . We then compare them to the corresponding scaling laws displayed in Table 4.

The plots shown in Figure 5 are obtained for the fixed value  $\varepsilon = 1$  and of the exponents  $i_3 \geq i_2 \geq i_1 \geq 1$ . The triple integral displays a similar qualitative behaviour as the analytic results in Table 4, again denoted by the red circles, for small values of  $-p$ . In fact, in Figure 5a, b, e and f, corresponding to Case 1, Case 2, Case 5, and Case 6 of the mentioned table, they display a slope of value  $-1 + \frac{1}{i_3}$ . The red circles in Figure 5c and g, corresponding to Case 3 and Case 7, have values

$$\log_{10}(-p) \left(-1 + \frac{1}{i_3}\right) + \log_{10}(-\log_{10}(-p)) + c,$$

for distinct constants  $c$ . The red circles presented in Figure 5d, corresponding to Case 4, are equal to

$$\log_{10}(-p) \left(-1 + \frac{1}{i_3}\right) + 2\log_{10}(-\log_{10}(-p)) + c$$

and those displayed in Figure 5h, corresponding to Case 8, are

$$3\log_{10}(-\log_{10}(-p)) + c,$$

for a different constant  $c$  each.

### 7 Applications

The early warning signs introduced in Theorems 3.3, 4.5 and 4.7 can be applied to a wide range of applications. As described in Example 5.2, the study of reaction-diffusion equations can be achieved through Fourier transforms. In particular, we consider linearisations of reaction-diffusion systems in the form (1.2). For a distance  $p$  to the bifurcation threshold, the solution of the linearised system on a stable solution  $u_*(p)$  behaves similarly to the solution of the original equation [24]. This is implied by the fact that the solution remains in the basin of attraction in finite time with high probability due to the strong dissipative effect of the linear term until  $p$  has crossed the bifurcation point.

The current section examines the relevance of our results to different models. Furthermore, their implementation in the prediction of real-life scenarios is discussed.

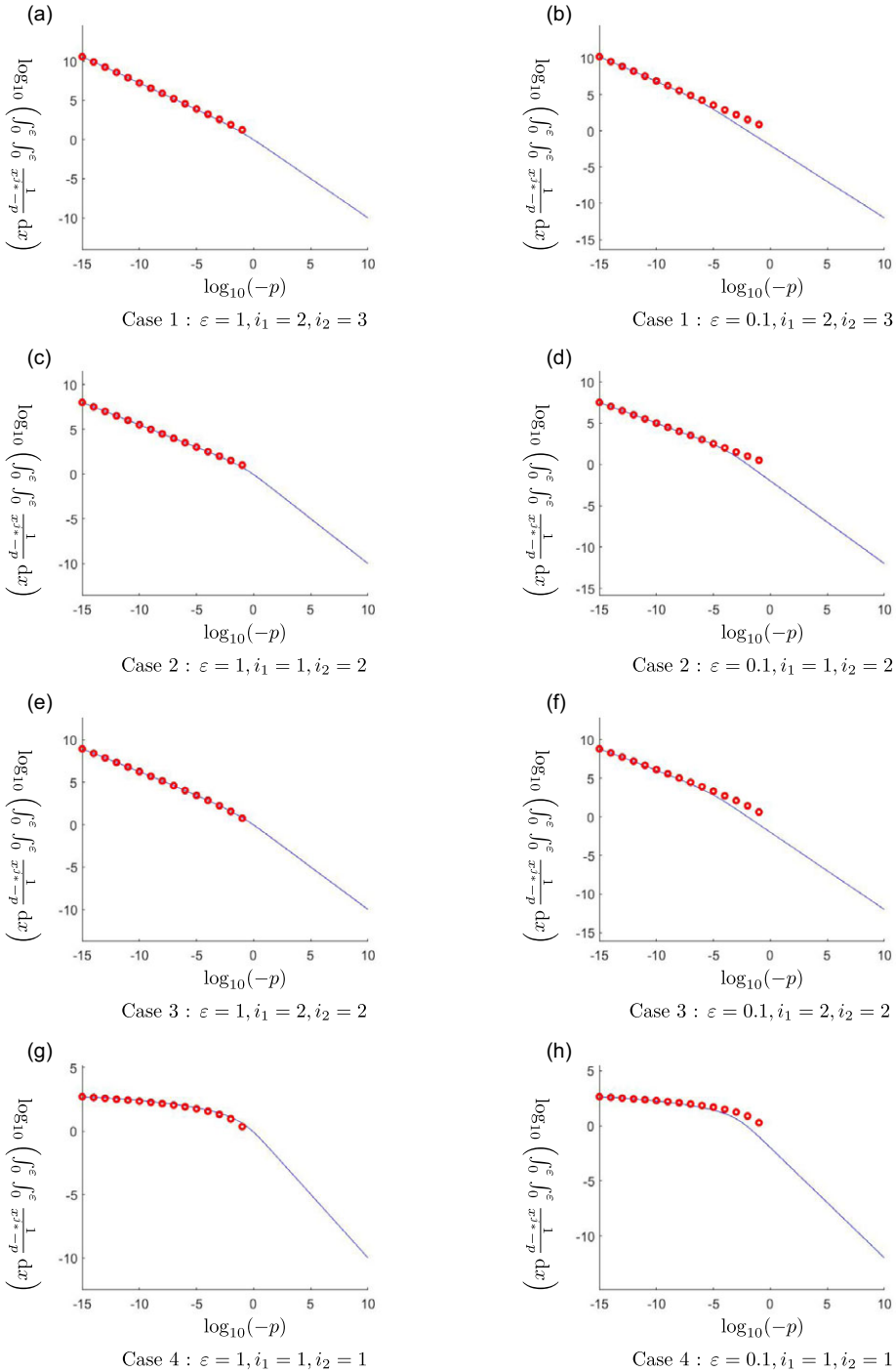


**Figure 4.** The solid lines describe the scaling law of the upper bound for the two-dimensional problem, illustrated by  $\log_{10}\left(\int_0^\epsilon \int_0^\epsilon \frac{1}{x^{i_1} y^{i_2}} dx\right)$  and decreasing  $\log_{10}(-p)$  with  $x = (x_1, x_2)$  and  $j_* = (i_1, i_2)$ . The numbering of the cases refers to Table 3. The circle lines serve as comparison with the corresponding scaling law presented in the table as an argument of  $\log_{10}$ .

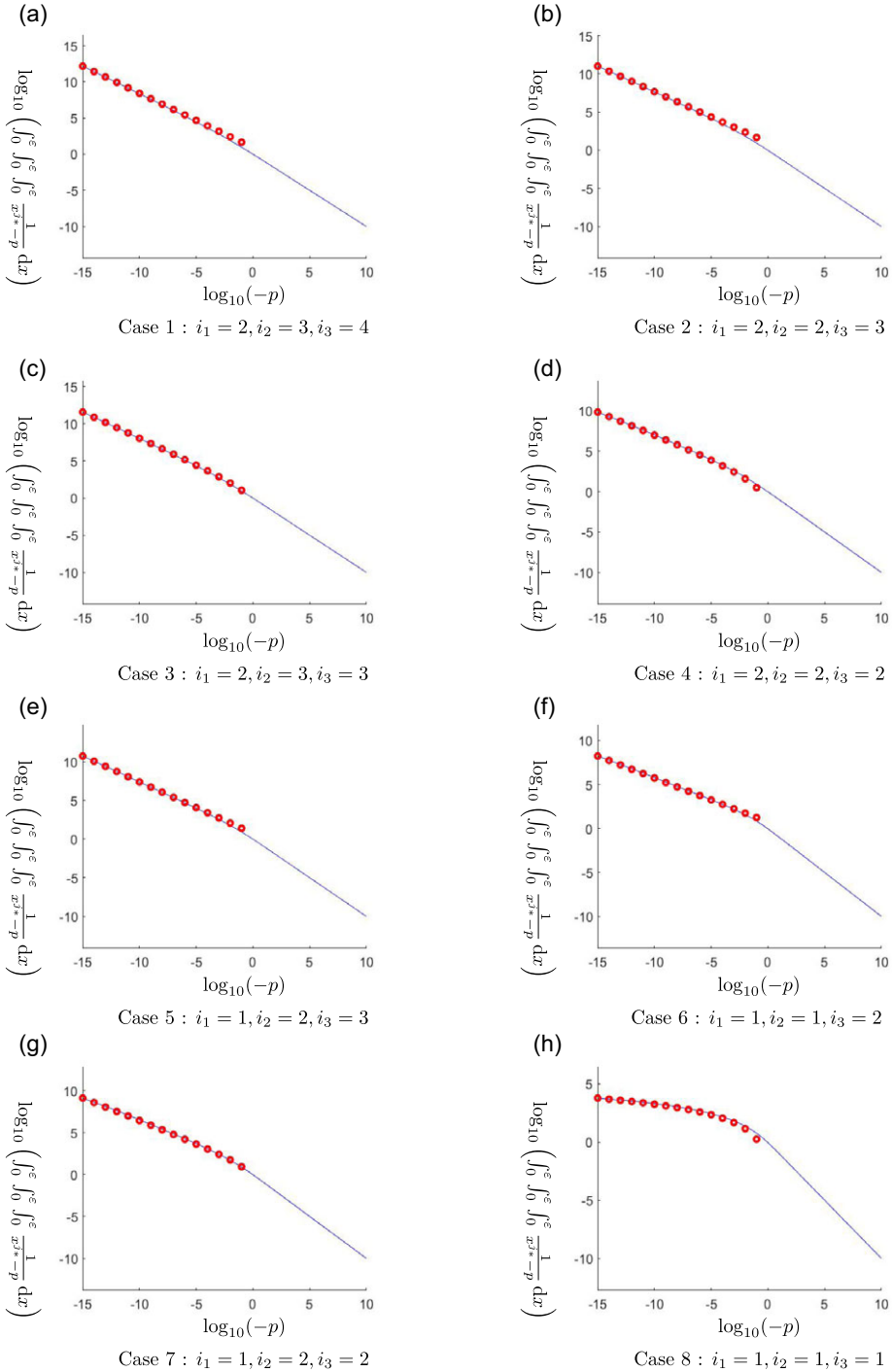


**Figure 5.** The solid lines describe the scaling law of the upper bound for the three-dimensional problem illustrated by  $\log_{10} \left( \int_0^{\epsilon} \int_0^{\epsilon} \int_0^{\epsilon} \frac{1}{x_1^{i_1} x_2^{i_2} x_3^{i_3}} dx \right)$  and decreasing  $\log_{10}(-p)$  with  $x = (x_1, x_2, x_3)$  and  $j_* = (i_1, i_2, i_3)$ . The numbering of cases refers to Table 4. The circle lines serve as comparison with the corresponding scaling law presented in the table as an argument of  $\log_{10}$ .

▷ First, we introduce the Ginzburg–Landau, Allen–Cahn, or Chafee–Infante equation,

$$du = (\partial_x^2 u + pu - u^3)dt,$$

in the domain  $\mathcal{X} = [-L, L]$  and Dirichlet boundary conditions. It finds applications in phase-ordering kinetic [8], quantum mechanics [22], and climate science [29]. The model is known to present a pitchfork supercritical bifurcation threshold at the parameter value  $p = 0$  [11]. The introduction of additive Gaussian noise is justified by the presence of lesser components in the physical model that can be treated as small stochastic perturbations [7, 57]. We also consider the domain in the limit  $L \rightarrow \infty$ , in order to study large spaces. In such a limit, the spectrum of  $\partial_x^2$  is continuous and the only stable solution for  $p < 0$  is the null function  $u_* = 0$ . The linearised system (1.2) is given with the drift operator

$$A(p) = \partial_x^2 + p \quad . \tag{7.1}$$

Example 5.2 implies that the time-asymptotic variance along almost any function  $g \in \mathcal{H}^2(\mathbb{R})$  yields a rate of divergence of order  $\Theta\left((-p)^{\frac{1}{2}}\right)$  as  $p \rightarrow 0^-$ . In Figure 6a, a numerical approximation of the time-asymptotic variance of a solution of (5.2) for (7.1) is displayed. The observable is considered along  $g = \mathcal{F}^{-1} \mathbb{1}_{[-0.25, 0.25]}$  and exhibits a slope of  $-\frac{1}{2}$  in a logarithmic scale, for  $p$  close to 0.

▷ We now consider the one-dimensional complex Ginzburg–Landau equation,

$$du = (\partial_x^2 u + (p + i)u - (-1 + i0, 1)|u|^2 u - |u|^4 u)dt,$$

for  $i$  the imaginary unit and  $|\cdot|$  the absolute value, in the domain  $\mathcal{X} = [-L, L]$  and Neumann boundary conditions. Similar to its real counterpart, the introduction of white additive noise is justified by minor components in the system [31]. For finite values of  $L$ , it is known that a supercritical Hopf bifurcation occurs at the stable solution  $u_* = 0$  in the limit  $p \rightarrow 0^-$  [62]. The assumption of the limit  $L \rightarrow +\infty$  follows from the observation of large domains in relevant applications and via the justification of the Ginzburg–Landau equation as an amplitude/modulation equation. The linearised system on  $u_* = 0$ , (1.2) with linear operator

$$A(p) = \partial_x^2 + p + i, \tag{7.2}$$

can be treated in Fourier space following Example 5.2 and the fourth generalisation in Section 5. In detail, for any  $g \in \mathcal{H}^2(\mathbb{R}; \mathbb{C})$  it holds

$$\begin{aligned} \langle g, V_\infty g \rangle &= \sigma^2 \int_0^\infty \langle e^{tA(p)} e^{tA(p)*} g, g \rangle dt = \sigma^2 \int_0^\infty \int_{\mathbb{R}} \overline{g(x)} e^{t(\partial_x^2 + p - i)} e^{t(\partial_x^2 + p + i)} g(x) dx dt \\ &= \sigma^2 \int_0^\infty \|e^{t(\partial_x^2 + p)} g\|^2 dt = \sigma^2 \int_0^\infty \|\mathcal{F}^{-1} e^{t(T_{-k^2} + p)} \mathcal{F} g\|^2 dt \\ &= \Theta\left(\int_0^\infty \|e^{t(T_{-k^2} + p)} \mathcal{F} g\|^2 dt\right) = \Theta\left(-\int_{\mathbb{R}} |\mathcal{F} g(k)|^2 \frac{1}{2(-k^2 + p)} dk\right). \end{aligned}$$

The time-asymptotic variance of the solution of the linearised system along almost any  $g \in \mathcal{H}^2(\mathbb{R}; \mathbb{C})$  is therefore characterised by rate  $\Theta\left((-p)^{-\frac{1}{2}}\right)$  as  $p \rightarrow 0^-$ . In Figure 6b, an approximation of the observable along  $g = \mathcal{F}^{-1} \mathbb{1}_{[-0.25, 0.25]}$  displays a slope of  $-\frac{1}{2}$  in a logarithmic scale, as  $p$  approaches 0. An example of fields with which the complex Ginzburg–Landau equation is associated is the research on thin superconductors [52]. The stochastic non-linear Ginzburg–Landau equation in dimension  $N > 1$  is ill-defined in the classical sense under the assumption of perturbation by white noise and requires renormalisation; yet, note that the linearised SPDEs we work with here are always well-defined, even with space-time white noise. Assuming the covariance operator  $Q$ , in (2.3), such that a solution for such equation exists [16, Theorems 5.20 and 7.13], an upper bound to the rate of divergence of the time-asymptotic variance of the solution of the linearised system can be obtained following Theorems 4.5, 4.7 and the third generalisation in Section 5.

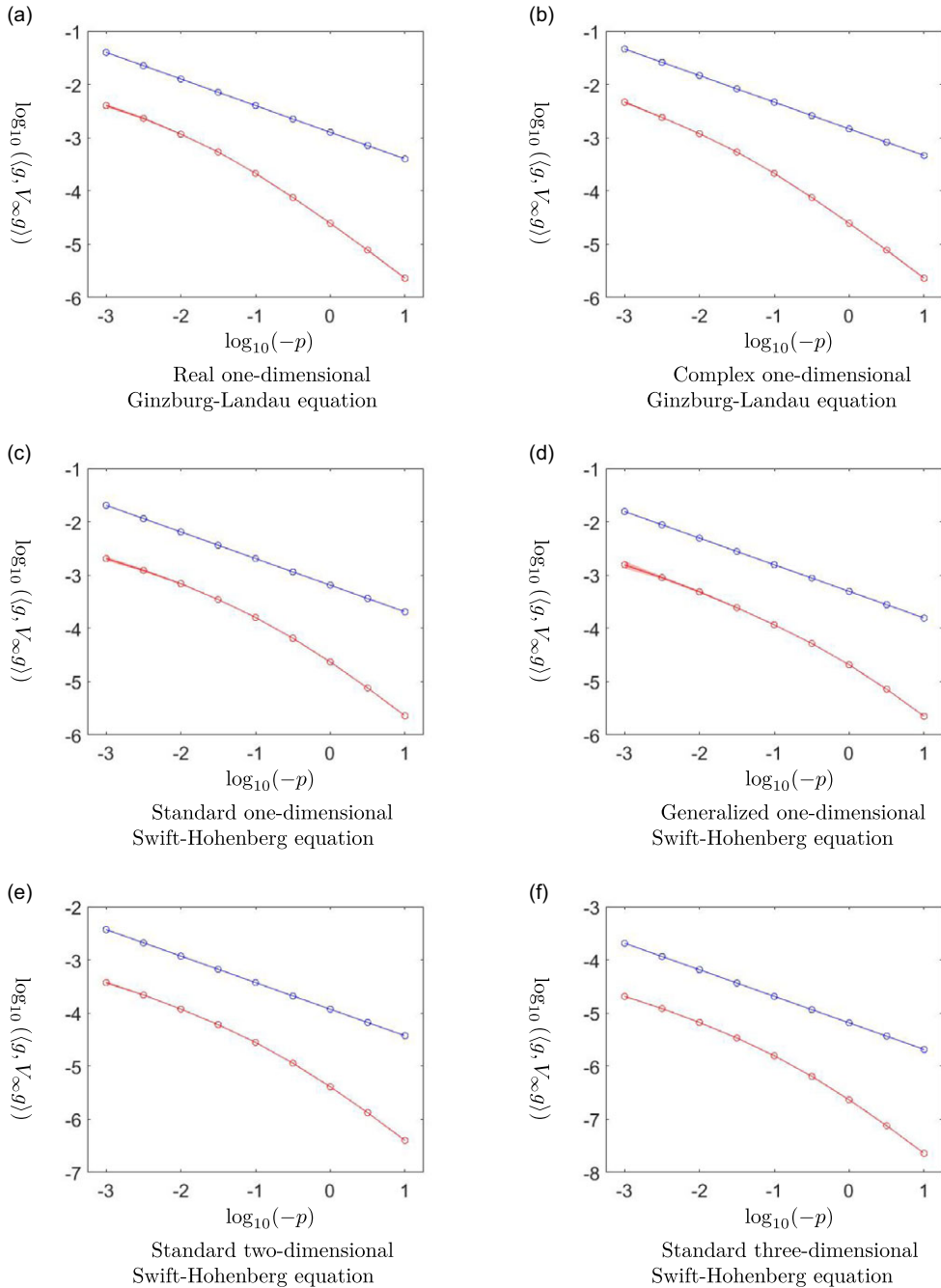


**Figure 6.** A numerical approximation of the time-asymptotic variance of the solution of (5.2) along the function  $g$  is displayed for different models discussed in Section 7 in a log-log plot. The figures are obtained following the method in Section 6 in Fourier space, for  $T = 10^4$ ,  $\delta t = 0.01$  and  $Q = 1$ . The red lines refer to the mean values of the observable for 10 sample solution, different for noise realisation. The areas have a width equal to double the corresponding numerical standard deviation. In Figure a, the drift term is described by (7.1); in Figure b, it is associated to (7.2); in Figure c to (7.3); in Figure d to (7.4); in Figure e to (7.5); in Figure f to (7.6). The respective functions  $g$  are introduced in Section 7. In blue, a line with a slope equal to  $-\frac{1}{2}$  is included as a comparison. In all figures, the lines appear to align for small values of  $p$ .



▷ Another equation of interest is the (standard) one-dimensional Swift–Hohenberg equation [9, 10, 34],

$$du = -(1 + \partial_x^2)^2 u + pu - u^3 dt,$$

with domain  $\mathcal{X} = \mathbb{R}$ . Such a deterministic equation is known to display Turing bifurcations [32, 33]. We insert a white-noise term, meant to simulate the effect of minor physical components, in the system [27]; in fact, the stochastic Swift–Hohenberg equation has been studied very frequently already in the context of amplitude equations. The linearisation of such an SPDE on the trivial solution  $u_*(x) = 0$ , for any  $x \in \mathbb{R}$ , takes the form of (5.2) with  $u_0 \in \mathcal{H}^4(\mathbb{R})$ ,  $Q = I$  and  $A : \mathcal{H}^4(\mathbb{R}) \rightarrow L^2(\mathbb{R})$  such that

$$Ag(x) = -(1 + \partial_x^2)^2 g(x), \tag{7.3}$$

for any  $g \in \mathcal{H}^4(\mathbb{R})$ . Example 5.2 can easily be generalised on such self-adjoint linear differential operators through Theorem 3.3. The scaling law of the variance of such a solution along  $g$  in a dense subset of  $\mathcal{H}^4(\mathbb{R})$  is given, therefore, by

$$\langle g, V_\infty g \rangle = \sigma^2 \int_0^\infty \langle e^{t(A+p)} e^{t(A+p)} g, g \rangle dt = \Theta \left( \int_0^\infty \|e^{t(T_f+p)} \mathcal{F}g\|^2 dt \right),$$

with  $f(k) = -(1 - k^2)^2$  for any  $k \in \mathbb{R}$ . From the Taylor expansion of  $f$  at  $k = \pm 1$ , it follows that the rate of divergence presents order  $\Theta \left( (-p)^{-\frac{1}{2}} \right)$ . The time-asymptotic variance of the linearised model is displayed in red in the log-log plot in Figure 6c. As described in Section 5, the variance along  $g = \mathcal{F}^{-1} \mathbb{1}_{[0.75, 1.25]}$  displays the rate of divergence  $\Theta \left( (-p)^{-\frac{1}{2}} \right)$  as  $p \rightarrow 0^-$ . The Swift–Hohenberg equation on large or unbounded domains [6] can be obtained from the Boussinesq approximation for fluid dynamics [60]. In such an application, the ergodic theory states that the figure displays the rate of divergence of the time-asymptotic variance of the projection of the rescaled fluid velocity  $u$  on the function  $g$  up to the proximity to a bifurcation threshold. In particular, Theorem 3.3 asserts that an equivalent order of divergence is assumed for  $g$  in a large set of indicator functions in  $L^2(\mathcal{X})$ . Therefore, it validates the study of the variance solely in bounded regions of space. As an example from [26], another practical use of the corresponding early warning sign is the prediction of sudden changes in the electric field in crystal optical fibre resonators implied by the change of a bifurcation parameter. In this case, the generalised Swift–Hohenberg equation linearised on  $u_* = 0$  yields

$$A = -\frac{\beta^2}{4} + \beta \partial_x^2 + \beta' \partial_x^3 - \partial_x^4 \tag{7.4}$$

and the variable  $u$  represents the deviation of the electric field from its value at the bifurcation threshold. Upon consideration of the variational equation, i.e.,  $\beta' = 0$ , the rate of the early warning sign can be obtained from Example 5.2. Set  $\beta < 0$  and  $g(x) = \mathcal{F}^{-1} \mathbb{1}_{[a,b]}$  for  $a < b$ , the scaling law of the time-asymptotic variance of the solution of the linearised system (1.2) on  $u_* = 0$  along  $g$  is given by

$$\langle g, V_\infty g \rangle = \sigma^2 \int_0^\infty \langle e^{t(A+p)} e^{t(A+p)} g, g \rangle dt = \Theta \left( \int_0^\infty \|e^{t(T_f+p)} \mathcal{F}g\|^2 dt \right),$$

with  $f(k) = -k^2(\beta + k^2) - \frac{\beta^2}{4}$  for any  $k \in \mathbb{R}$ . The function  $f$  has multiple roots, and the corresponding equation presents an example of the first generalisation in Section 5. The values  $k_* = \pm \left( -\frac{\beta}{2} \right)^{\frac{1}{2}}$  are global maxima of  $f$  and solutions of order 2. Therefore, the scaling law of the time-asymptotic variance of the solution of the linearised equation along  $g$  is

$$\langle g, V_\infty g \rangle = \begin{cases} \Theta \left( (-p)^{-\frac{1}{2}} \right) & , \text{ for } a < -\left( -\frac{\beta}{2} \right)^{\frac{1}{2}} < b \text{ or } a < \left( -\frac{\beta}{2} \right)^{\frac{1}{2}} < b, \\ \Theta(1) & , \text{ otherwise,} \end{cases}$$

for  $p \rightarrow 0^-$ . In Figure 6d, the time-asymptotic variance of the solution of (5.2) along the function  $g = \mathcal{F}^{-1} \mathbb{1}_{\left[(-\frac{\beta}{2})^{\frac{1}{2}} - 0.25, (-\frac{\beta}{2})^{\frac{1}{2}} + 0.25\right]}$  is displayed in red on logarithmic scale. Under the assumption

$\beta = -1$ , the variance appears to diverge with order  $\Theta\left((-p)^{-\frac{1}{2}}\right)$  in the limit  $p \rightarrow 0^-$ . Among other instances, the (standard) Swift–Hohenberg equation finds further applications in chemistry [54] and in hydrodynamics [56].

▷ We also consider the application of Theorem 3.3 to the standard two-dimensional Swift–Hohenberg equation. For more general versions whose linearisation presents a self-adjoint operator, Theorem 4.5 and Example 5.2 provide an upper bound to the rate of the time-asymptotic variance of the solution of the linearised system. Such equations hold particular interest in the field of hydrodynamics as they enable a simulation of the Rayleigh–Bénard convection phenomena in non-Boussinesq fluids [60, 67] and of the Taylor–Couette flow [30, 56]. A generalisation of the two-dimensional Swift–Hohenberg equation has also been employed in optics [44, 45]. The standard two-dimensional Swift–Hohenberg equation can be studied similarly to its one-dimensional equivalent. It is of the form

$$du = \left(-1 + \partial_{x_1}^2 + \partial_{x_2}^2\right)u + pu - u^3 dt,$$

on domain  $\mathcal{X} = \mathbb{R}^2$ . Again, we insert an additive noise component [27] and consider only the linearised SPDE along the deterministic stable solution  $u_* = 0$ , which presents a valid approximation of the standard equation for values of the bifurcation parameter suitably distant to the bifurcation threshold. We set  $A : \mathcal{H}^4(\mathbb{R}^2) \rightarrow L^2(\mathbb{R}^2)$  as the Swift–Hohenberg operator on two spatial dimensions, i.e.,

$$Ag(x) = -\left(1 + \partial_{x_1}^2 + \partial_{x_2}^2\right)g(x), \tag{7.5}$$

for any  $g \in \mathcal{H}^4(\mathbb{R}^2)$  and  $x = (x_1, x_2)$ . We study the variance of the solution of (5.2) for  $u_0 \in \mathcal{H}^4(\mathbb{R}^2)$ ,  $p < 0$  and  $Q$  a bounded operator with bounded inverse. We consider  $g \in \mathcal{H}^4(\mathbb{R}^2)$  and  $f_i(k) = k_i$  for  $i \in \{1, 2\}$  and  $k = (k_1, k_2) \in \mathbb{R}^2$ . Let  $\mathcal{F}$  denote the Fourier transform on  $L^2(\mathbb{R}^2)$  and  $\hat{g} = \mathcal{F}g$ . It follows that

$$\begin{aligned} \langle g, V_\infty g \rangle &= \sigma^2 \int_0^\infty \langle e^{t(A+p)} Q e^{t(A+p)} g, g \rangle dt = \Theta \left( \int_0^\infty \|e^{t(A+p)} g\|^2 dt \right) \\ &= \Theta \left( \int_0^\infty \left\| \mathcal{F}^{-1} e^{t\left(\mathbb{T}_{-(1-r_1^2-r_2^2)}\right)^2+p} \mathcal{F}g \right\|^2 dt \right) = \Theta \left( \int_0^\infty \left\| e^{t\left(\mathbb{T}_{-(1-r_1^2-r_2^2)}\right)^2+p} \hat{g} \right\|^2 dt \right). \end{aligned}$$

We know that the scaling law as  $p \rightarrow 0^-$  of such a scalar product is equivalent for a dense set of functions  $g$  in  $\mathcal{H}^4(\mathbb{R}^2)$ . From such a set we can choose  $g$  such that  $\hat{g} = \mathbb{1}_D$ , where  $D$  denotes the circle of radius  $\sqrt{2}$  centred at the origin in  $\mathbb{R}^2$ . Through Fubini’s Theorem, we can study the integral on polar spatial coordinates as

$$\int_0^\infty \iint_D e^{t\left(-\left(1-k_1^2-k_2^2\right)^2+p\right)} dk dt = \iint_D \frac{1}{\left(1-k_1^2-k_2^2\right)^2-p} dk = \int_0^{2\pi} \int_0^{\sqrt{2}} \frac{r}{\left(1-r^2\right)^2-p} dr d\theta.$$

Introducing  $r' = 1 - r^2$  and  $r'' = r'(-p)^{-\frac{1}{2}}$  we can use the substitution method and obtain

$$\int_0^{2\pi} \int_0^{\sqrt{2}} \frac{r}{\left(1-r^2\right)^2-p} dr d\theta = \pi \int_{-1}^1 \frac{1}{r'^2-p} dr' = (-p)^{-\frac{1}{2}} \int_{-(-p)^{-\frac{1}{2}}}^{(-p)^{-\frac{1}{2}}} \frac{1}{r''^2+1} dr'' = \Theta \left( (-p)^{-\frac{1}{2}} \right).$$

Figure 6e displays the time-asymptotic variance of a solution of (5.2) along a function  $g$  in red on a logarithmic scale. In such a case, we consider  $g = \mathcal{F}^{-1} \mathbb{1}_{\hat{D}}$ , for  $\hat{D} \subset \mathbb{R}^2$  such that

$$\hat{D} = \left\{ (k_1, k_2) \in \mathbb{R}^2 \mid k_1 = r \sin(\theta), k_2 = r \cos(\theta), r \in [0.75, 1.25] \text{ and } \theta \in \left[ -\frac{\pi}{36}, \frac{\pi}{36} \right] \right\}.$$

The observable exhibits the scaling law  $\Theta\left((-p)^{-\frac{1}{2}}\right)$  as  $p$  approaches the bifurcation threshold.

▷ Similarly to the previous application, we consider the three-dimensional Swift–Hohenberg equation. It is used in various applications, including hydrodynamics [30, 60]. For solutions of generalised versions whose linearisation leads to a self-adjoint operator in the drift component, upper bounds to the time-asymptotic variance of the solution of the linearised equation can be obtained through Theorem 4.7 and Example 5.2.

The standard three-dimensional Swift–Hohenberg equation is of the form

$$du = \left( - (1 + \partial_{x_1}^2 + \partial_{x_2}^2 + \partial_{x_3}^2)u + pu - u^3 \right) dt,$$

on domain  $\mathcal{X} = \mathbb{R}^3$ . The linearised SPDE on  $u_* = 0$  with additive Gaussian noise is characterised by the drift operator  $A : \mathcal{H}^4(\mathbb{R}^3) \rightarrow L^2(\mathbb{R}^3)$  of the form

$$Ag(x) = - (1 + \partial_{x_1}^2 + \partial_{x_2}^2 + \partial_{x_3}^2) g(x), \tag{7.6}$$

for any  $g \in \mathcal{H}^4(\mathbb{R}^3)$  and  $x = (x_1, x_2, x_3)$ . We study the time-asymptotic variance of the solution of (5.2) for initial condition  $u_0 \in \mathcal{H}^4(\mathbb{R}^3)$ ,  $p < 0$  and  $Q$  a bounded operator with bounded inverse. We consider  $g \in \mathcal{H}^4(\mathbb{R}^3)$  and  $f_i(k) = k_i$  for  $i \in \{1, 2, 3\}$  and  $k = (k_1, k_2, k_3) \in \mathbb{R}^3$ . Again, let  $\mathcal{F}$  refer to the Fourier transform on  $L^2(\mathbb{R}^3)$  and  $\hat{g} = \mathcal{F}g$ . It follows that

$$\begin{aligned} \langle g, V_\infty g \rangle &= \sigma^2 \int_0^\infty \langle e^{t(A+p)} Q e^{t(A+p)} g, g \rangle dt = \Theta \left( \int_0^\infty \|e^{t(A+p)} g\|^2 dt \right) \\ &= \Theta \left( \int_0^\infty \left\| \mathcal{F}^{-1} e^{t \left( \mathbb{T} - (1-f_1^2 - f_2^2 - f_3^2)^2 + p \right)} \mathcal{F} g \right\|^2 dt \right) = \Theta \left( \int_0^\infty \left\| e^{t \left( \mathbb{T} - (1-f_1^2 - f_2^2 - f_3^2)^2 + p \right)} \hat{g} \right\|^2 dt \right). \end{aligned}$$

We know that the scaling law as  $p \rightarrow 0^-$  of such scalar product is equivalent for a dense set of functions  $g$  in  $\mathcal{H}^4(\mathbb{R}^3)$ . From such set we can choose  $g$  such that  $\hat{g} = \mathbb{1}_S$ , where  $S$  denotes the sphere of radius  $\sqrt{2}$  centred at the origin in  $\mathbb{R}^3$ . Through Fubini’s Theorem, we can study the integral on spherical spatial coordinates as

$$\begin{aligned} \int_0^\infty \iiint_S e^{t \left( \mathbb{T} - (1-k_1^2 - k_2^2 - k_3^2)^2 + p \right)} dk dt &= \iiint_S \frac{1}{(1 - k_1^2 - k_2^2 - k_3^2)^2 - p} dk \\ &= \int_0^\pi \int_0^{2\pi} \int_0^{\sqrt{2}} \frac{r^2 \sin(\phi)}{(1 - r^2)^2 - p} dr d\theta d\phi = 4\pi \int_0^{\sqrt{2}} \frac{r^2}{(1 - r^2)^2 - p} dr = \Theta \left( (-p)^{-\frac{1}{2}} \right). \end{aligned}$$

Figure 6f displays the time-asymptotic variance of a solution of (5.2) along a function  $g$  in red on a logarithmic scale. We consider  $g = \mathcal{F}^{-1} \mathbb{1}_S$ , for  $\hat{S} \subset \mathbb{R}^3$  such that

$$\begin{aligned} \hat{S} &= \left\{ (k_1, k_2) \in \mathbb{R}^2 \mid k_1 = r \sin(\theta) \sin(\phi), k_2 = r \sin(\theta) \cos(\phi), k_3 = r \cos(\theta), \right. \\ &\quad \left. r \in [0.75, 1.25] \text{ and } \theta, \phi \in \left[ -\frac{\pi}{36}, \frac{\pi}{36} \right] \right\}. \end{aligned}$$

The observable shows a slope of  $-\frac{1}{2}$  in logarithmic scale for  $p \rightarrow 0^-$ .

▷ Yet another class of SPDEs arising in applications where our results apply are systems of reaction-diffusion equations that model various applications. A famous example is the (one-dimensional) FitzHugh–Nagumo model [2]. Among the applications to such a model is the study of activators and inhibitors in anisotropic systems [4], with interest in fluid mechanics [37] and medicine [66]. Recently, the inclusion of an additive stochastic term in the system and its reduced version, the Nagumo equation of the form

$$du = (\Delta u + pu + u(1 - u)(u - a) + v) dt$$

with  $\Delta$  the Laplace operator and  $v$  a space-heterogeneous term has been examined [12, 13, 21, 61] along with the assumption of unbounded domains  $\mathcal{X} = \mathbb{R}$  [64]. As an example, the presence of noise is justified in the application of neurophysiology by the effect of random input current in neurons of

synaptic or external nature [61]. Under such assumptions, the reduced equation is of a generalised space-heterogeneous Ginzburg–Landau form, which can be treated similarly. In fact, Theorem 3.3 provides the corresponding rate of the time-asymptotic variance of the solution of the linearised equation previous to a pitchfork [11] or saddle-node [42] bifurcation. Given the stable solution  $u_*(p)$ , such an equation is of the form (1.2) and also gives a Schrödinger operator

$$A(p) = \Delta + p - a + 2(1 + a)u_*(p) - 3u_*(p)^2.$$

The dependence of  $u_*$  on  $p$  affects the spectrum of  $A(p)$  because it introduces heterogeneity in space. The scaling law is described analytically in Example 5.3. Unless  $u_*$  is a constant function,  $A(p)$  is not diagonalised in Fourier space, which leads to substantial additional numerical difficulties. Hence, we do not explore the numerical observation of the variance of a solution of the linearised model for  $u_*$  non-constant in this work and leave it for future work. For the case  $a = v(x) = u_*(x) = 0$  for any  $x \in \mathbb{R}$ , we refer to Figure 6a, where the time-asymptotic variance along  $g = \mathbb{1}_{[-0.25, 0.25]}$  displays a rate of divergence of order  $\Theta\left((-p)^{\frac{1}{2}}\right)$  as  $p$  approaches 0.

▷ As discussed in Section 5, the generalisations of Theorems 3.3, 4.5 and 4.7 are not restricted to unbounded domains. This is the case for certain more complex models with linear operators  $A(p)$ , such as certain Schrödinger operators with electric and magnetic potentials [36]. We also note that, for large domains and  $N = 1$ , the proximity of eigenvalues of differential operators with discrete spectrum, such as the Laplace operator, can delay the hyperbolic divergence of the early warning sign in reaction-diffusion equations discussed in Remark 5.4. An example of an application to such a case can be found in climate science in different two-dimensional ocean models, which display supercritical pitchfork and saddle-node bifurcations [3, 19].

## 8 Conclusion and outlook

We have studied the time-asymptotic covariance operator of the system (2.1) along certain types of functions  $g \in L^2(\mathcal{X})$ , i.e.,  $\langle g, V_\infty g \rangle$ . Our results contribute to the study of early warning signs for the qualitative change that arises as the parameter  $p < 0$  in (2.1) approaches 0 from below. A critical role for the behaviour of the early warning sign is given to the values assumed by the non-positive function  $f: \mathcal{X} \subseteq \mathbb{R}^N \rightarrow \mathbb{R}$ , in (2.1), in the neighbourhood of one of its roots, labelled as  $x_*$ .

We have found sharp scaling laws for locally analytic functions  $f$  on a one-dimensional domain by utilising the tool function  $f_\alpha(x)$ . For the two- and three-dimensional cases, we have studied the asymptotic behaviour of upper bounds of  $\langle g, V_\infty g \rangle$ . For general dimensions  $N$ , we have found convergence in the variance for certain functions  $f$ . In these cases, the search for a finer early warning sign that provides more information might be useful.

Our results can be applied to a wide range of models in which critical transitions and bifurcations are present. A more detailed application of the theory is currently a work in progress for a large-scale model in climate science.

In future work, a novel route could be the study of similar early warning sign problems for different types of operators, such as linear differential operators that are not self-adjoint. Another promising research direction is to aim to determine weaker assumptions on the linear operators present in (5.2) or assuming unbounded  $g$  on  $x_*$  for  $N > 1$ . The results for one-dimensional and higher-dimensional domains have been proven for analytic functions  $f$ . A deeper discussion on multiplication operators with functions that do not behave locally like polynomials could be of further interest. Lastly, the results obtained in the paper, as tables listing rates, could be the basis for an induction method to extend the study to  $N > 3$ .

**Financial support.** This project has received funding from the European Union’s Horizon 2020 research and innovation programme under Grant Agreement 956170.

**Competing interest.** The authors declare none.

## References

- [1] Alley, R. B., Marotzke, J., Nordhaus, W. D., et al. (2003) Abrupt climate change. *Science* **299** (5615), 2005–2010.
- [2] Asgari, Y., Ghaemi, M. & Mahjani, M. G. (2011) Pattern formation of the fitzhugh-nagumo model: Cellular automata approach. *Iran. J. Chem. Chem. Eng.*
- [3] Baars, S., Viebahn, J., Mulder, T. E., Kuehn, C., Wubs, F. W. & Dijkstra, H. A. (2017) Continuation of probability density functions using a generalized lyapunov approach. *J. Comput. Phys.* **336**, 627–643.
- [4] Bär, M., Meron, E. & Utzny, C. (2002) Pattern formation on anisotropic and heterogeneous catalytic surfaces. *Chaos* **12** (1), 204–214.
- [5] Bernuzzi, P. & Kuehn, C. (2023) Bifurcations and early-warning signs for spdes with spatial heterogeneity. *J. Dyn. Differ. Equations*, 1–45.
- [6] Blömker, D., Hairer, M. & Pavliotis, G. (2005) Modulation equations: Stochastic bifurcation in large domains. *Comm. Math. Phys.* **258**, 479–512.
- [7] Blumenthal, A., Engel, M. & Neamtu, A. (2021) On the pitchfork bifurcation for the chafee-infante equation with additive noise, arXiv preprint arXiv: 2108.11073.
- [8] Bray, A. J. (2002) Theory of phase-ordering kinetics. *Adv. Phys.* **51**(2), 481–587.
- [9] Burke, J. & Knobloch, E. (2007) Homoclinic snaking: Structure and stability. *Chaos* **17** (3).
- [10] Burke, J. & Knobloch, E. (2007) Snakes and ladders: Localized states in the Swift–Hohenberg equation. *Phys. Rev. A* **360** (6), 681–688.
- [11] Chafee, N. & Infante, E. F. (1974) A bifurcation problem for a nonlinear partial differential equation of parabolic type. *Appl. Anal.* **4** (1), 17–37.
- [12] Cordoni, F. & Di Persio, L. (2017) Optimal control for the stochastic fitzhugh-nagumo model with recovery variable, arXiv preprint arXiv: 1705.10227.
- [13] Cordoni, F. & Persio, L. D. (2021) Optimal control of the fitzhugh–nagumo stochastic model with nonlinear diffusion. *Appl. Math. Optim.*, 1–22.
- [14] Cotilla-Sanchez, E., Hines, P. D. & Danforth, C. M. (2012) Predicting critical transitions from time series synchrophasor data. *IEEE Trans. Smart Grid* **3** (4), 1832–1840.
- [15] Crauel, H. & Flandoli, F. (1998) Additive noise destroys a pitchfork bifurcation. *J. Dyn. Differ. Equations* **10**, 259–274.
- [16] Da Prato, G. & Zabczyk, J. (1992). *Stochastic Equations in Infinite Dimensions*, Cambridge University Press.
- [17] Dakos, V., Scheffer, M., van Nes, E., Brovkin, V., Petoukhov, V. & Held, H. (2008) Slowing down as an early warning signal for abrupt climate change. *Proc. Natl. Acad. Sci. USA* **105** (38), 14308–14312.
- [18] Deift, P. & Killip, R. (1999) On the absolutely continuous spectrum of one-dimensional schrödinger operators with square summable potentials. *Comm. Math. Phys.* **203**, 341–347.
- [19] Dijkstra, H. A. & Molemaker, M. J. (1997) Symmetry breaking and overturning oscillations in thermohaline-driven flows. *J. Fluid Mech.* **331**, 169–198.
- [20] Ditlevsen, P. & Johnsen, S. (2010) Tipping points: Early warning and wishful thinking. *Geophys. Res. Lett.* **37**, 19703.
- [21] Eichinger, K., Gnann, M. V. & Kuehn, C. (2022) Multiscale analysis for traveling-pulse solutions to the stochastic Fitzhugh–Nagumo equations. *Ann. Appl. Probab.* **32** (5), 3229–3282.
- [22] Faris, W. G. & Jona-Lasinio, G. (1982) Large fluctuations for a nonlinear heat equation with noise. *J. Phys. A Math. Theor.* **15** (10), 3025.
- [23] Gnann, M., Kuehn, C. & Pein, A. (2019) Towards sample path estimates for fast-slow SPDEs. *Eur. J. Appl. Math.* **30** (5), 1004–1024.
- [24] Gowda, K. & Kuehn, C. (2015) Early-warning signs for pattern-formation in stochastic partial differential equations. *Commun. Nonlinear Sci. Numer. Simul.* **22** (1), 55–69.
- [25] Hall, B. C. (2013). *Quantum Theory for Mathematicians*, New York, NY, Springer.
- [26] Hariz, A., Bahloul, L., Cherbi, L., et al. (2019) Swift-Hohenberg equation with third-order dispersion for optical fiber resonators. *Phys. Rev. A* **100** (2), 023816.
- [27] Hernández-García, E., San Miguel, M., Toral, R., Vi, J., et al. (1992) Noise and pattern selection in the one-dimensional Swift-Hohenberg equation. *Phys. D* **61** (1-4), 159–165.
- [28] Higham, D. J. (2001) An algorithmic introduction to numerical simulation of stochastic differential equations. *SIAM Rev.* **43** (3), 525–546.
- [29] Högele, M. A. (2011) Metastability of the chafee-infante equation with small heavy-tailed lévy noise. Humboldt-Universität zu Berlin, Mathematisch-Naturwissenschaftliche Fakultät II.
- [30] Hohenberg, P. & Swift, J. (1992) Effects of additive noise at the onset of Rayleigh–Bénard convection. *Phys. Rev. A* **46** (8), 4773.
- [31] Hoshino, M., Inahama, Y. & Naganuma, N. (2017) Stochastic complex ginzburg-landau equation with space-time white noise. arXiv preprint arXiv: 1702.07062.
- [32] Hummel, F., Jelbart, S. & Kuehn, C. (2022) Geometric blow-up of a dynamic turing instability in the swift-hohenberg equation. arXiv preprint arXiv: 2207.03967.
- [33] Jelbart, S. & Kuehn, C. (2023) A formal geometric blow-up method for pattern forming systems. arXiv preprint arXiv: 2302.06343.
- [34] Kao, H.-C., Beaume, C. & Knobloch, E. (2014) Spatial localization in heterogeneous systems. *Phys. Rev. E* **89** (1), 012903.
- [35] Knuth, D. E. (1976) Big omicron and big omega and big theta. *ACM Sigact News* **8** (2), 18–24.
- [36] Korotyayev, E. & Saburova, N. (2021) On continuous spectrum of magnetic schrödinger operators on periodic discrete graphs. arXiv preprint arXiv: 2101.05571.

- [37] Kramer, L. & Pesch, W. (1995) Convection instabilities in nematic liquid crystals. *Annu. Rev. Fluid Mech.* **27** (1), 515–539.
- [38] Kuehn, C. (2008) Scaling of saddle-node bifurcations: Degeneracies and rapid quantitative changes. *J. Phys. A* **42** (4), 9–17.
- [39] Kuehn, C. (2011) A mathematical framework for critical transitions: Bifurcations, fast–slow systems and stochastic dynamics. *Phys. D* **240** (12), 1020–1035.
- [40] Kuehn, C. (2013) A mathematical framework for critical transitions: Normal forms, variance and applications. *J. Nonlinear Sci.* **23**, 457–510.
- [41] Kuehn, C. (2015) *Multiple Time Scale Dynamics*, Cham, Springer, Vol. **191**.
- [42] Kuehn, C. (2015) Numerical continuation and spde stability for the 2d cubic–quintic allen–cahn equation. *SIAM-ASA J. Uncertain. Quantif.* **3** (1), 762–789.
- [43] Kuehn, C. & Romano, F. (2019) Scaling laws and warning signs for bifurcations of spdes. *Eur. J. Appl. Math.* **30** (5), 853–868.
- [44] Lega, J., Moloney, J. & Newell, A. (1994) Swift-Hohenberg equation for lasers. *Phys. Rev. Lett.* **73** (22), 2978.
- [45] Lega, J., Moloney, J. & Newell, A. (1995) Universal description of laser dynamics near threshold. *Phys. D* **83** (4), 478–498.
- [46] Lenton, T. M. (2011) Early warning of climate tipping points. *Nat. Clim. Change* **1** (4), 201–209.
- [47] Lord, G. J., Powell, C. E. & Shardlow, T. (2014) *An Introduction to Computational Stochastic Pdes*, New York, NY, Cambridge University Press, Vol. **50**.
- [48] May, R. M., Levin, S. A. & Sugihara, G. (2008) Ecology for bankers. *Nature* **451** (7181), 893–894.
- [49] McSharry, P. E., Smith, L. A. & Tarasenko, L. (2003) Prediction of epileptic seizures: Are nonlinear methods relevant? *Nat. Med.* **9** (3), 241–242.
- [50] Meisel, C. & Kuehn, C. (2012) Scaling effects and spatio-temporal multilevel dynamics in epileptic seizures. *PLoS One* **7** (2), 1–11.
- [51] Mezzadri, F. (2006) How to generate random matrices from the classical compact groups. arXiv preprint math-ph/0609050.
- [52] Milošević, M. & Geurts, R. (2010) The ginzburg–landau theory in application. *Phys. C* **470** (19), 791–795.
- [53] Mormann, F., Andrzejak, R. G., Elger, C. E. & Lehnertz, K. (2006) Seizure prediction: The long and winding road. *Brain* **130** (2), 314–333.
- [54] M’F, H., Métens, S., Borckmans, P. & Dewel, G. (1995) Pattern selection in the generalized swift-hohenberg model. *Phys. Rev. E* **51** (3), 2046.
- [55] O’Regan, S. M. & Drake, J. M. (2013) Theory of early warning signals of disease emergence and leading indicators of elimination. *Theor. Ecol.* **6**, 333–357.
- [56] Pomeau, Y. & Manneville, P. (1980) Wavelength selection in cellular flows. *Phys. Lett. A* **75** (4), 296–298.
- [57] Rolland, J., Bouchet, F. & Simonnet, E. (2016) Computing transition rates for the 1-d stochastic Ginzburg–Landau–Allen–Cahn equation for finite-amplitude noise with a rare event algorithm. *J. Stat. Phys.* **162**, 277–311.
- [58] Scheffer, M., Bascompte, J., Brock, W. A., et al. (2009) Early-warning signals for critical transitions. *Nature* **461** (7260), 53–59.
- [59] Scheffer, M., Carpenter, S., Foley, J. A., Folke, C. & Walker, B. (2001) Catastrophic shifts in ecosystems. *Nature* **413** (6856), 591–596.
- [60] Swift, J. & Hohenberg, P. C. (1977) Hydrodynamic fluctuations at the convective instability. *Phys. Rev. A* **15** (1), 319.
- [61] Tuckwell, H. C. (1992) Random perturbations of the reduced Fitzhugh–Nagumo equation. *Phys. Scr.* **46** (6), 481.
- [62] Uecker, H. (2021) *Numerical Continuation and Bifurcation in Nonlinear PDEs*, Philadelphia, PA, SIAM.
- [63] Venegas, J. G., Winkler, T., Musch, G., et al. (2005) Self-organized patchiness in asthma as a prelude to catastrophic shifts. *Nature* **434** (7034), 777–782.
- [64] Wang, B. (2009) Random attractors for the stochastic Fitzhugh–Nagumo system on unbounded domains. *Nonlinear Anal. Theory Methods Appl.* **71** (7–8), 2811–2828.
- [65] Wiesenfeld, K. (1985) Noisy precursors of nonlinear instabilities. *J. Stat. Phys.* **38** (5), 1071–1097.
- [66] Winfree, A. (1997) Heart muscle as a reaction–diffusion medium: The roles of electric potential diffusion, activation front curvature, and anisotropy. *Int. J. Bifurc. Chaos Appl. Sci. Eng.* **7** (03), 487–526.
- [67] Xi, H.-w., Gunton, J. & Vinals, J. (1993) Pattern formation during rayleigh–bénard convection in non-boussinesq fluids. arXiv preprint patt-sol/9305001.

## Appendix A: Proof Theorem 4.5

The following proof justifies the description of the scaling law of the upper bound presented in Theorem 4.5, and its results are summarised in Table 3. The proof is based upon a splitting of the upper bound into two summands, labeled as  $\mathfrak{A}$  and  $\mathfrak{B}$ , the first of which is studied similarly to the methods employed in the proof of Theorem 3.1.

**Proof Theorem 4.5** Up to permutation of indices, we assume  $i_2 \geq i_1 \geq 1$  for simplicity. We also set  $\varepsilon = 1$ , up to rescaling of the space variable  $x$  and subsequently of  $\mathcal{X}$ . Lemma 4.3 implies for a positive

constant  $C > 0$  that

$$\langle g, V_\infty g \rangle \leq \frac{1}{C} \int_0^1 \int_0^1 \frac{1}{x_1^{i_1} x_2^{i_2} - p} dx_2 dx_1 = \frac{-1}{Cp} \int_0^1 \int_0^1 \frac{1}{(x_1(-p))^{-\frac{1}{2i_1}} (x_2(-p))^{-\frac{1}{2i_2}} + 1} dx_2 dx_1 .$$

For convenience, we will write  $q := -p > 0$ . Through integration by substitution with  $y_n := x_n q^{-\frac{1}{2i_n}}$  for  $n \in \{1, 2\}$  we obtain

$$\begin{aligned} \langle g, V_\infty g \rangle &\leq \frac{1}{Cq} \int_0^1 \int_0^1 \frac{1}{(x_1 q^{-\frac{1}{2i_1}})^{i_1} (x_2 q^{-\frac{1}{2i_2}})^{i_2} + 1} dy_2 dy_1 & (A1) \\ &= \frac{1}{C} q^{-1+\frac{1}{2}(\frac{1}{i_1}+\frac{1}{i_2})} \int_0^q \int_0^q \frac{1}{y_1^{i_1} y_2^{i_2} + 1} dy_2 dy_1 . \end{aligned}$$

We evaluate the integral by substituting  $z = \frac{1}{y_1^{i_1} y_2^{i_2} + 1}$  to get

$$\begin{aligned} \langle g, V_\infty g \rangle &\leq \frac{1}{C} q^{-1+\frac{1}{2}(\frac{1}{i_1}+\frac{1}{i_2})} \int_0^q \int_0^q \frac{1}{y_1^{i_1} y_2^{i_2} + 1} dy_2 dy_1 \\ &= \frac{1}{C} q^{-1+\frac{1}{2}(\frac{1}{i_1}+\frac{1}{i_2})} \int_0^q \int_{\frac{1}{y_1^{i_1} q^{-\frac{1}{2}+1}}^1} z z^{-2} \frac{1}{i_2} \left(\frac{1}{z} - 1\right)^{\frac{1}{i_2}-1} y_1^{-\frac{i_1}{i_2}} dz dy_1 & (A2) \\ &= \frac{1}{C} q^{-1+\frac{1}{2}(\frac{1}{i_1}+\frac{1}{i_2})} \int_0^q \left( \frac{q^{-\frac{1}{2i_2}}}{y_1^{i_1} q^{-\frac{1}{2}+1} + 1} + \int_{\frac{1}{y_1^{i_1} q^{-\frac{1}{2}+1}}^1 \left(\frac{1}{z} - 1\right)^{\frac{1}{i_2}-1} y_1^{-\frac{i_1}{i_2}} dz \right) dy_1 \\ &= \frac{1}{C} q^{-1+\frac{1}{2i_1}} \underbrace{\int_0^q \frac{1}{y_1^{i_1} q^{-\frac{1}{2}+1}} dy_1}_{\mathfrak{A}} + \frac{1}{C} q^{-1+\frac{1}{2}(\frac{1}{i_1}+\frac{1}{i_2})} \underbrace{\int_0^q \int_{\frac{1}{y_1^{i_1} q^{-\frac{1}{2}+1}}^1 \left(\frac{1}{z} - 1\right)^{\frac{1}{i_2}-1} y_1^{-\frac{i_1}{i_2}} dz dy_1}_{\mathfrak{B}} . \end{aligned}$$

In the following, we first analyse  $\mathfrak{A}$  before evaluating the order of divergence of  $\mathfrak{B}$ . Further, as seen above, the choice of  $i_1$  and  $i_2$  dictates the rate of the upper bound. Hence, we consider different cases corresponding to the choice of values of  $i_1$  and  $i_2$ , whose numbering is displayed in Table 3.

◇ Scaling law of  $\mathfrak{A}$  in Cases 1 and 3. Note that the order of  $\mathfrak{A}$  is independent of  $i_2$ , which simplifies the study of its scaling law. We start by discussing  $\mathfrak{A}$  for  $i_2 \geq i_1 > 1$ . Through the substitution  $y'_1 = y_1 q^{-\frac{1}{2i_1}}$  it follows that

$$\mathfrak{A} = q^{-1+\frac{1}{i_1}} \int_0^{q^{-\frac{1}{i_1}}} \frac{1}{y_1^{i_1} + 1} dy'_1 .$$

As already established in (3.5), the integral is converging for  $p \rightarrow 0^-$ , and therefore we find a rate of divergence for the first summand given by

$$\Theta \left( (-p)^{-1+\frac{1}{i_1}} \right) \tag{A3}$$

for  $p \rightarrow 0^-$  and  $i_2 \geq i_1 > 1$ .

◇ Scaling law of  $\mathfrak{A}$  in Cases 2 and 4. Next, we consider  $\mathfrak{A}$  assuming that  $i_2 \geq i_1 = 1$ . Through the same substitutions present in the previous case, we get

$$\mathfrak{A} = \int_0^{q^{-1}} \frac{1}{y'_1 + 1} dy'_1 = \log (q^{-1} + 1) .$$

This component diverges for  $q$  approaching zero from above. For  $i_2 \geq i_1 = 1$ , it follows that

$$\Theta \left( \log \left( (-p)^{-1} \right) \right) = \Theta \left( -\log \left( -p \right) \right) \tag{A4}$$

is the rate of divergence for  $p$  approaching zero from below.

◇ Scaling law of  $\mathfrak{B}$  in Case 1. We consider the case  $i_2 > i_1 > 1$ . In regard to  $\mathfrak{B}$ , our first goal is to switch integrals for more convenient computation. Through Fubini’s Theorem, we obtain

$$\begin{aligned} \mathfrak{B} &= q^{-1+\frac{1}{2}\left(\frac{1}{i_1}+\frac{1}{i_2}\right)} \int_{\frac{1}{q-1+1}}^1 \int_{\left(\frac{1}{z}-1\right)^{\frac{1}{i_1}} q^{\frac{1}{2i_1}}}^{q^{-\frac{1}{2i_1}}} \left(\frac{1}{z}-1\right)^{\frac{1}{2}} y_1^{-\frac{i_1}{2}} dy_1 dz \\ &= q^{-1+\frac{1}{2}\left(\frac{1}{i_1}+\frac{1}{i_2}\right)} \int_{\frac{1}{q-1+1}}^1 \left(\frac{1}{z}-1\right)^{\frac{1}{2}} \left[ \frac{1}{\left(1-\frac{i_1}{i_2}\right)} y_1^{-\frac{i_1}{2}+1} \right]_{\left(\frac{1}{z}-1\right)^{\frac{1}{i_1}} q^{\frac{1}{2i_1}}}^{q^{-\frac{1}{2i_1}}} dz \\ &= \frac{q^{-1+\frac{1}{2}\left(\frac{1}{i_1}+\frac{1}{i_2}\right)}}{1-\frac{i_1}{i_2}} \int_{\frac{1}{q-1+1}}^1 \left(\frac{1}{z}-1\right)^{\frac{1}{2}} \left( q^{\frac{1}{2i_2}-\frac{1}{2i_1}} - \left(\frac{1}{z}-1\right)^{\frac{1}{i_1}-\frac{1}{i_2}} q^{\frac{1}{2i_1}-\frac{1}{2i_2}} \right) dz \\ &= \left(1-\frac{i_1}{i_2}\right)^{-1} \left( q^{-1+\frac{1}{2}} \int_{\frac{1}{q-1+1}}^1 \left(\frac{1}{z}-1\right)^{\frac{1}{2}} dz - q^{-1+\frac{1}{i_1}} \int_{\frac{1}{q-1+1}}^1 \left(\frac{1}{z}-1\right)^{\frac{1}{i_1}} dz \right). \end{aligned} \tag{A5}$$

By substitution with  $z' = \frac{1}{z} - 1$ , we obtain

$$\mathfrak{B} = \left(1-\frac{i_1}{i_2}\right)^{-1} \left( q^{-1+\frac{1}{2}} \int_0^{q^{-1}} \frac{z'^{\frac{1}{2}}}{(z'+1)^2} dz' - q^{-1+\frac{1}{i_1}} \int_0^{q^{-1}} \frac{z'^{\frac{1}{i_1}}}{(z'+1)^2} dz' \right). \tag{A6}$$

Given  $i_2 > i_1 > 1$ , the integrals in (A6) can be uniformly bounded for any  $q > 0$ . Hence, we find that for  $\mathfrak{B}$  the rate of divergence is given by

$$\Theta \left( q^{-1+\frac{1}{2}} \right) - \Theta \left( q^{-1+\frac{1}{i_1}} \right) = \Theta \left( (-p)^{-1+\frac{1}{2}} \right) - \Theta \left( (-p)^{-1+\frac{1}{i_1}} \right) = \Theta \left( (-p)^{-1+\frac{1}{2}} \right)$$

as  $p$  approaches zero from below. From (A2), we get the rate of divergence of the upper bound as

$$\Theta \left( (-p)^{-1+\frac{1}{i_1}} \right) + \Theta \left( (-p)^{-1+\frac{1}{2}} \right) = \Theta \left( (-p)^{-1+\frac{1}{2}} \right).$$

for  $i_2 > i_1 > 1$ .

◇ Scaling law of  $\mathfrak{B}$  in Case 2. We suppose now that  $i_2 > i_1 = 1$ . We can follow the steps in the case above, up to (A6). We then note that

$$\int_0^{q^{-1}} \frac{z'}{(z'+1)^2} dz' = \log(q^{-1}+1) + \frac{1}{q^{-1}+1} - 1. \tag{A7}$$

Therefore, we obtain that  $\mathfrak{B}$  diverges with rate

$$\Theta \left( (-p)^{-1+\frac{1}{2}} \right) - \Theta \left( \log((-p)^{-1}) \right) = \Theta \left( (-p)^{-1+\frac{1}{2}} \right),$$

for  $p \rightarrow 0^-$ . Combining this result with equation (A4) we obtain for  $i_2 > i_1 = 1$  an overall rate of divergence of order

$$\Theta \left( -\log(-p) \right) + \Theta \left( (-p)^{-1+\frac{1}{2}} \right) = \Theta \left( (-p)^{-1+\frac{1}{2}} \right).$$



◇ Scaling law of  $\mathfrak{B}$  in Case 3. For the third case we consider  $\mathfrak{B}$  with  $i_2 = i_1 = i > 1$ , for which we get

$$\begin{aligned} \mathfrak{B} &= q^{-1+\frac{1}{i}} \int_{\frac{1}{q^{-1+i}}}^1 \int_{\left(\frac{1}{z}-1\right)^{\frac{1}{i}} q^{\frac{1}{2i}}}^{q^{-\frac{1}{2i}}} \left(\frac{1}{z}-1\right)^{\frac{1}{i}} y_1^{-1} dy_1 dz \\ &= q^{-1+\frac{1}{i}} \int_{\frac{1}{q^{-1+i}}}^1 \left(\frac{1}{z}-1\right)^{\frac{1}{i}} \left(\log\left(q^{-\frac{1}{2i}}\right) - \log\left(\left(\frac{1}{z}-1\right)^{\frac{1}{i}} q^{\frac{1}{2i}}\right)\right) dz \\ &= q^{-1+\frac{1}{i}} \left(-\frac{\log(q)}{i} \int_{\frac{1}{q^{-1+i}}}^1 \left(\frac{1}{z}-1\right)^{\frac{1}{i}} dz - \frac{1}{i} \int_{\frac{1}{q^{-1+i}}}^1 \left(\frac{1}{z}-1\right)^{\frac{1}{i}} \log\left(\frac{1}{z}-1\right) dz\right). \end{aligned}$$

Again, we substitute  $z' = \frac{1}{z} - 1$  to get

$$\mathfrak{B} = q^{-1+\frac{1}{i}} \left(-\frac{\log(q)}{i} \int_0^{q^{-1}} \frac{z'^{\frac{1}{i}}}{(z'+1)^2} dz' - \frac{1}{i} \int_0^{q^{-1}} \frac{z'^{\frac{1}{i}} \log(z')}{(z'+1)^2} dz'\right). \tag{A8}$$

The integrals in (A8) are uniformly bounded for any  $q > 0$  due to  $i > 1$ . Equation (A8) implies that  $\mathfrak{B}$  assumes, in this case, rate of divergence

$$\Theta\left(-(-p)^{-1+\frac{1}{i}} \log(-p)\right) + \Theta\left((-p)^{-1+\frac{1}{i}}\right) = \Theta\left(-(-p)^{-1+\frac{1}{i}} \log(-p)\right)$$

for  $p \rightarrow 0^-$ . From (A2) and (A3), we get that the rate of divergence of the upper bound is

$$\Theta\left((-p)^{-1+\frac{1}{i}}\right) + \Theta\left(-(-p)^{-1+\frac{1}{i}} \log(-p)\right) = \Theta\left(-(-p)^{-1+\frac{1}{i}} \log(-p)\right).$$

◇ Scaling law of  $\mathfrak{B}$  in Case 4. In the last case, we suppose that  $i_2 = i_1 = i = 1$ . Hence, (A8) assumes the form

$$\begin{aligned} \mathfrak{B} &= -\log(q) \int_0^{q^{-1}} \frac{z'}{(z'+1)^2} dz' - \int_0^{q^{-1}} \frac{z' \log(z')}{(z'+1)^2} dz' \\ &= -\log(q) \left(\log(q^{-1} + 1) + \frac{1}{q^{-1} + 1} - 1\right) - \int_0^{q^{-1}} \frac{z' \log(z')}{(z'+1)^2} dz'. \end{aligned} \tag{A9}$$

We obtain therefore from (A9) and (C3), in Appendix C, that the two leading terms in  $\mathfrak{B}$  diverge respectively as  $\log^2(q)$  and as  $-\frac{1}{2} \log^2(q)$ . Hence, we know that the divergence of  $\mathfrak{B}$  presents rate

$$\Theta(\log^2(-p)) \quad \text{for } p \rightarrow 0^-.$$

Combining such result with the rate of divergence of  $\mathfrak{A}$  in (A4), we obtain

$$\Theta(-\log(-p)) + \Theta(\log^2(-p)) = \Theta(\log^2(-p)) \quad \text{for } p \rightarrow 0^-,$$

as an overall upper bound for  $i_2 = i_1 = 1$ .

□

### Appendix B: Proof Theorem 4.7

The subsequent proof validates the description of the rate of divergence of the upper bound discussed in Theorem 4.7 and in Table 4. The approach is similar to the one involved in the proof of Theorem 4.5 as the upper bound is split into two summands, labeled  $\mathfrak{C}$  and  $\mathfrak{D}$ . The first summand is studied similarly to the upper bound in the stated proof for the two-dimensional case.

**Proof Theorem 4.7** Lemma 4.3 implies that

$$\langle g, V_\infty g \rangle \leq \frac{\sigma^2}{2C} \int_0^\varepsilon \int_0^\varepsilon \int_0^\varepsilon \frac{1}{x_1^{i_1} x_2^{i_2} x_3^{i_3} - p} dx_3 dx_2 dx_1$$

for a constant  $C > 0$  and any  $p < 0$ . As in the two-dimensional case, we make use of  $q := -p > 0$  and we fix  $\varepsilon = 1$ , up to rescaling of the spatial variable  $x$ . Up to permutation of the indices we consider  $i_3 \geq i_2 \geq i_1 \geq 1$ , thus excluding the cases described in Remark 4.4.

We follow a similar computation of the integral as in Theorem 4.5. First, we study it in the coordinates  $y_n = x_n q^{-\frac{1}{3i_n}}$  for all  $n \in \{1, 2, 3\}$  and then we substitute  $y_3$  with  $z = \frac{1}{y_1^i y_2^i y_3^i + 1}$  to obtain

$$\begin{aligned} & \int_0^1 \int_0^1 \int_0^1 \frac{1}{x_1^{i_1} x_2^{i_2} x_3^{i_3} + q} dx_3 dx_2 dx_1 \\ &= q^{-1+\frac{1}{3}(\frac{1}{i_1}+\frac{1}{i_2}+\frac{1}{i_3})} \int_0^q q^{-\frac{1}{3i_1}} \int_0^q q^{-\frac{1}{3i_2}} \int_0^q q^{-\frac{1}{3i_3}} \frac{1}{y_1^{i_1} y_2^{i_2} y_3^{i_3} + 1} dy_3 dy_2 dy_1 \\ &= q^{-1+\frac{1}{3}(\frac{1}{i_1}+\frac{1}{i_2}+\frac{1}{i_3})} \int_0^q q^{-\frac{1}{3i_1}} \int_0^q q^{-\frac{1}{3i_2}} \int_{\frac{1}{y_1^{i_1} y_2^{i_2} q^{-\frac{1}{3}+1}}}^1 zz^{-2} \frac{1}{i_3} \left(\frac{1}{z} - 1\right)^{\frac{1}{i_3}-1} y_1^{-\frac{i_1}{i_3}} y_2^{-\frac{i_2}{i_3}} dz dy_2 dy_1. \end{aligned}$$

Through integration by parts on the inner integral, it follows that

$$\begin{aligned} & \int_0^1 \int_0^1 \int_0^1 \frac{1}{x_1^{i_1} x_2^{i_2} x_3^{i_3} + q} dx_3 dx_2 dx_1 \\ &= \underbrace{q^{-1+\frac{1}{3}(\frac{1}{i_1}+\frac{1}{i_2})} \int_0^q q^{-\frac{1}{3i_1}} \int_0^q q^{-\frac{1}{3i_2}} \frac{1}{y_1^{i_1} y_2^{i_2} q^{-\frac{1}{3}+1}} dy_2 dy_1}_{\mathfrak{C}} \tag{B1} \\ &+ \underbrace{q^{-1+\frac{1}{3}(\frac{1}{i_1}+\frac{1}{i_2}+\frac{1}{i_3})} \int_0^q q^{-\frac{1}{3i_1}} \int_0^q q^{-\frac{1}{3i_2}} \int_{\frac{1}{y_1^{i_1} y_2^{i_2} q^{-\frac{1}{3}+1}}}^1 \left(\frac{1}{z} - 1\right)^{\frac{1}{i_3}} y_1^{-\frac{i_1}{i_3}} y_2^{-\frac{i_2}{i_3}} dz dy_2 dy_1}_{\mathfrak{D}}. \end{aligned}$$

We study each summand independently as in Theorem 4.5. Further, we distinguish between different choices of values for  $i_n$  for  $n \in \{1, 2, 3\}$ . We find the scaling laws of  $\mathfrak{C}$ ,  $\mathfrak{D}$ , and the overall upper bound for each case. The numbering of the cases is reported in Table 4.

◇ Scaling law of  $\mathfrak{C}$  in Cases 1–8. We assume  $i_1, i_2, i_3 > 0$ . We change the variables in the integral with  $y'_n = y_n q^{-\frac{1}{6i_n}}$  for  $n \in \{1, 2\}$  to have

$$\begin{aligned} & q^{-1+\frac{1}{3}(\frac{1}{i_1}+\frac{1}{i_2})} \int_0^q q^{-\frac{1}{3i_1}} \int_0^q q^{-\frac{1}{3i_2}} \frac{1}{(y_1 q^{-\frac{1}{6i_1}})^{i_1} (y_2 q^{-\frac{1}{6i_2}})^{i_2} + 1} dy_2 dy_1 \\ &= q^{-1+\frac{1}{2}(\frac{1}{i_1}+\frac{1}{i_2})} \int_0^q q^{-\frac{1}{2i_1}} \int_0^q q^{-\frac{1}{2i_2}} \frac{1}{y_1^{i_1} y_2^{i_2} + 1}. \end{aligned}$$

We note that this expression is equivalent to the integral given by (A1), as  $i_3$  does not affect such a rate of divergence. Hence, we have proven the divergence of  $\mathfrak{C}$  for different choices of  $i_1, i_2$  and that its corresponding rate is displayed in Table 3.

◆ Scaling law of  $\mathfrak{D}$  in Case 1. Next, we continue analyzing the component  $\mathfrak{D}$  of (B1). First, we assume that  $i_3 > i_2 > i_1 > 1$ . We change the order of integrals through Fubini’s Theorem, placing the

integral on  $z$  in the outer position and obtaining

$$\begin{aligned}
 & q^{-1+\frac{1}{3}(\frac{1}{i_1}+\frac{1}{i_2}+\frac{1}{i_3})} \int_0^q \int_0^{q^{-\frac{1}{3i_1}}} \int_0^{q^{-\frac{1}{3i_2}}} \int_{\frac{1}{y_1^{i_1} y_2^{i_2} q^{-\frac{1}{3}+1}}}^1 \left(\frac{1}{z} - 1\right)^{\frac{1}{i_3}} y_1^{-\frac{i_1}{i_3}} y_2^{-\frac{i_2}{i_3}} dz dy_2 dy_1 \tag{B2} \\
 & = q^{-1+\frac{1}{3}(\frac{1}{i_1}+\frac{1}{i_2}+\frac{1}{i_3})} \int_{\frac{1}{q^{-1+1}}}^1 \int_{(\frac{1}{z}-1)^{\frac{1}{i_1}} q^{\frac{2}{3i_1}}} \int_{(\frac{1}{z}-1)^{\frac{1}{i_2}} q^{\frac{1}{3i_2}} y_1^{-\frac{i_1}{i_2}}} \left(\frac{1}{z} - 1\right)^{\frac{1}{i_3}} y_1^{-\frac{i_1}{i_3}} y_2^{-\frac{i_2}{i_3}} dy_2 dy_1 dz.
 \end{aligned}$$

Since  $i_3 > i_2$ , it follows that  $\mathfrak{D}$  is equal to

$$\begin{aligned}
 & \left(-\frac{i_2}{i_3} + 1\right)^{-1} q^{-1+\frac{1}{3}(\frac{1}{i_1}+\frac{1}{i_2}+\frac{1}{i_3})} \int_{\frac{1}{q^{-1+1}}}^1 \int_{(\frac{1}{z}-1)^{\frac{1}{i_1}} q^{\frac{2}{3i_1}}} \left(\frac{1}{z} - 1\right)^{\frac{1}{i_3}} y_1^{-\frac{i_1}{i_3}} \left[ y_2^{-\frac{i_2}{i_3}+1} \right]_{y_2=(\frac{1}{z}-1)^{\frac{1}{i_2}} q^{\frac{1}{3i_2}} y_1^{-\frac{i_1}{i_2}}}^{q^{-\frac{1}{3i_2}}} dy_1 dz \\
 & = \underbrace{\left(-\frac{i_2}{i_3} + 1\right)^{-1} q^{-1+\frac{1}{3i_1}+\frac{2}{3i_3}} \int_{\frac{1}{q^{-1+1}}}^1 \left(\frac{1}{z} - 1\right)^{\frac{1}{i_3}} \int_{(\frac{1}{z}-1)^{\frac{1}{i_1}} q^{\frac{2}{3i_1}}} \int_{(\frac{1}{z}-1)^{\frac{1}{i_2}} q^{\frac{1}{3i_2}} y_1^{-\frac{i_1}{i_3}}} dy_1 dz}_{\mathfrak{D}.I} \tag{B3} \\
 & - \underbrace{\left(-\frac{i_2}{i_3} + 1\right)^{-1} q^{-1+\frac{1}{3i_1}+\frac{2}{3i_2}} \int_{\frac{1}{q^{-1+1}}}^1 \left(\frac{1}{z} - 1\right)^{\frac{1}{i_2}} \int_{(\frac{1}{z}-1)^{\frac{1}{i_1}} q^{\frac{2}{3i_1}}} y_1^{-\frac{i_1}{i_2}} dy_1 dz}_{\mathfrak{D}.II}.
 \end{aligned}$$

From  $i_3 > i_1$ , we know that  $\mathfrak{D}.I$  is equal to

$$\begin{aligned}
 & \left(-\frac{i_1}{i_3} + 1\right)^{-1} \left( q^{-1+\frac{1}{i_3}} \int_{\frac{1}{q^{-1+1}}}^1 \left(\frac{1}{z} - 1\right)^{\frac{1}{i_3}} dz - q^{-1+\frac{1}{i_1}} \int_{\frac{1}{q^{-1+1}}}^1 \left(\frac{1}{z} - 1\right)^{\frac{1}{i_1}} dz \right) \tag{B4} \\
 & = \left(-\frac{i_1}{i_3} + 1\right)^{-1} \left( \underbrace{q^{-1+\frac{1}{i_3}} \int_0^{q^{-1}} \frac{z'^{\frac{1}{i_3}}}{(z'+1)^2} dz'}_{\mathfrak{D}.I.1} - \underbrace{q^{-1+\frac{1}{i_1}} \int_0^{q^{-1}} \frac{z'^{\frac{1}{i_1}}}{(z'+1)^2} dz'}_{\mathfrak{D}.I.2} \right),
 \end{aligned}$$

with  $z' = \frac{1}{z} - 1$ . Equivalently, since  $i_2 > i_1$ , the summand  $\mathfrak{D}.II$  is equal to

$$\left(-\frac{i_1}{i_2} + 1\right)^{-1} \left( \underbrace{q^{-1+\frac{1}{i_2}} \int_0^{q^{-1}} \frac{z'^{\frac{1}{i_2}}}{(z'+1)^2} dz'}_{\mathfrak{D}.II.1} - \underbrace{q^{-1+\frac{1}{i_1}} \int_0^{q^{-1}} \frac{z'^{\frac{1}{i_1}}}{(z'+1)^2} dz'}_{\mathfrak{D}.II.2} \right).$$

For  $i_1, i_2, i_3 > 1$ , the integrals in  $\mathfrak{D}.I.1, \mathfrak{D}.I.2, \mathfrak{D}.II.1$  and  $\mathfrak{D}.II.2$  are uniformly bounded for any  $q > 0$ . Hence, the rate of divergence of  $\mathfrak{D}$  is

$$\Theta \left( (-p)^{-1+\frac{1}{i_3}} \right) - \Theta \left( (-p)^{-1+\frac{1}{i_1}} \right) - \Theta \left( (-p)^{-1+\frac{1}{i_2}} \right) + \Theta \left( (-p)^{-1+\frac{1}{i_1}} \right) = \Theta \left( (-p)^{-1+\frac{1}{i_3}} \right).$$

Combining the rates of  $\mathfrak{C}$  and  $\mathfrak{D}$ , we prove the divergence, for  $i_3 > i_2 > i_1 > 1$ , of the upper bound with scaling law

$$\Theta \left( (-p)^{-1+\frac{1}{i_2}} \right) + \Theta \left( (-p)^{-1+\frac{1}{i_3}} \right) = \Theta \left( (-p)^{-1+\frac{1}{i_3}} \right).$$

◆ Scaling law of  $\mathfrak{D}$  in Case 2. Next, we consider the case  $i_3 > i_2 = i_1 = i > 1$ . We can follow the same argumentation of the previous case until (B4) and prove that

$$\mathfrak{D}.I = \left(-\frac{i}{i_3} + 1\right)^{-1} (\mathfrak{D}.I.1 - \mathfrak{D}.I.2).$$

In this case, summand  $\mathfrak{D.II}$  is equal to

$$\begin{aligned}
 & q^{-1+\frac{1}{7}} \int_{\frac{1}{q-1+1}}^1 \left(\frac{1}{z}-1\right)^{\frac{1}{7}} \int_{\left(\frac{1}{z}-1\right)^{\frac{1}{7}} q^{\frac{2}{3i}}}^{q^{-\frac{1}{3i}}} y_1^{-1} dy_1 dz \\
 &= -\frac{1}{i} q^{-1+\frac{1}{7}} \int_{\frac{1}{q-1+1}}^1 \left(\frac{1}{z}-1\right)^{\frac{1}{7}} \left(\log(q) + \log\left(\frac{1}{z}-1\right)\right) dz \\
 &= -\frac{1}{i} q^{-1+\frac{1}{7}} \log(q) \underbrace{\int_0^{q^{-1}} \frac{z'^{\frac{1}{7}}}{(z'+1)^2} dz}_{\mathfrak{D.II.3}} - \frac{1}{i} q^{-1+\frac{1}{7}} \underbrace{\int_0^{q^{-1}} \frac{z'^{\frac{1}{7}} \log(z')}{(z'+1)^2} dz}_{\mathfrak{D.II.4}}.
 \end{aligned} \tag{B5}$$

The integrals in  $\mathfrak{D.II.3}$  and  $\mathfrak{D.II.4}$  are uniformly bounded for any  $q > 0$ , therefore the rate of divergence of  $\mathfrak{D.II}$  is  $\Theta\left(-(-p)^{1+\frac{1}{7}} \log(-p)\right)$ . The rate assumed by  $\mathfrak{D}$  is

$$\Theta\left((-p)^{-1+\frac{1}{15}}\right) - \Theta\left(-(-p)^{-1+\frac{1}{7}} \log(-p)\right) = \Theta\left((-p)^{-1+\frac{1}{15}}\right).$$

Overall, we find the rate of the upper bound in the case  $i_3 > i_2 = i_1 > 1$  to be

$$\Theta\left(-(-p)^{-1+\frac{1}{2}} \log(-p)\right) + \Theta\left((-p)^{-1+\frac{1}{15}}\right) = \Theta\left((-p)^{-1+\frac{1}{15}}\right).$$

◆ **Scaling law of  $\mathfrak{D}$  in Case 3.** Next, we consider the case  $i_3 = i_2 > i_1 > 1$ . We observe again equation (B2) and label  $i_3 = i_2 = i$  to obtain

$$\begin{aligned}
 & q^{-1+\frac{1}{3}\left(\frac{1}{i_1}+\frac{2}{7}\right)} \int_{\frac{1}{q-1+1}}^1 \int_{\left(\frac{1}{z}-1\right)^{\frac{1}{i_1}} q^{\frac{2}{3i_1}}}^{q^{-\frac{1}{3i_1}}} \int_{\left(\frac{1}{z}-1\right)^{\frac{1}{i_1}} q^{\frac{2}{3i_1}} y_1^{-\frac{i_1}{7}}}^{\left(\frac{1}{z}-1\right)^{\frac{1}{7}}} y_1^{-\frac{i_1}{7}} y_2^{-1} dy_2 dy_1 dz \\
 &= q^{-1+\frac{1}{3}\left(\frac{1}{i_1}+\frac{2}{7}\right)} \log\left(q^{-\frac{1}{3i_1}}\right) \int_{\frac{1}{q-1+1}}^1 \int_{\left(\frac{1}{z}-1\right)^{\frac{1}{i_1}} q^{\frac{2}{3i_1}}}^{q^{-\frac{1}{3i_1}}} \left(\frac{1}{z}-1\right)^{\frac{1}{7}} y_1^{-\frac{i_1}{7}} dy_1 dz \\
 &\quad - q^{-1+\frac{1}{3}\left(\frac{1}{i_1}+\frac{2}{7}\right)} \int_{\frac{1}{q-1+1}}^1 \int_{\left(\frac{1}{z}-1\right)^{\frac{1}{i_1}} q^{\frac{2}{3i_1}}}^{q^{-\frac{1}{3i_1}}} \left(\frac{1}{z}-1\right)^{\frac{1}{7}} y_1^{-\frac{i_1}{7}} \log\left(\left(\frac{1}{z}-1\right)^{\frac{1}{7}} q^{\frac{1}{3i_1}} y_1^{-\frac{i_1}{7}}\right) dy_1 dz \\
 &= -\frac{2}{3i} q^{-1+\frac{1}{3}\left(\frac{1}{i_1}+\frac{2}{7}\right)} \log(q) \underbrace{\int_{\frac{1}{q-1+1}}^1 \int_{\left(\frac{1}{z}-1\right)^{\frac{1}{i_1}} q^{\frac{2}{3i_1}}}^{q^{-\frac{1}{3i_1}}} \left(\frac{1}{z}-1\right)^{\frac{1}{7}} y_1^{-\frac{i_1}{7}} dy_1 dz}_{\mathfrak{D.III}} \\
 &\quad - \frac{1}{i} q^{-1+\frac{1}{3}\left(\frac{1}{i_1}+\frac{2}{7}\right)} \underbrace{\int_{\frac{1}{q-1+1}}^1 \int_{\left(\frac{1}{z}-1\right)^{\frac{1}{i_1}} q^{\frac{2}{3i_1}}}^{q^{-\frac{1}{3i_1}}} \left(\frac{1}{z}-1\right)^{\frac{1}{7}} \log\left(\frac{1}{z}-1\right) y_1^{-\frac{i_1}{7}} dy_1 dz}_{\mathfrak{D.IV}} \\
 &\quad + \frac{i_1}{i} q^{-1+\frac{1}{3}\left(\frac{1}{i_1}+\frac{2}{7}\right)} \underbrace{\int_{\frac{1}{q-1+1}}^1 \int_{\left(\frac{1}{z}-1\right)^{\frac{1}{i_1}} q^{\frac{2}{3i_1}}}^{q^{-\frac{1}{3i_1}}} \left(\frac{1}{z}-1\right)^{\frac{1}{7}} y_1^{-\frac{i_1}{7}} \log(y_1) dy_1 dz}_{\mathfrak{D.V}}.
 \end{aligned} \tag{B6}$$

First we evaluate  $\mathfrak{D}.III$  by integrating with respect to  $y_1$ . Since  $i > i_1$ , we get that  $\mathfrak{D}.III$  is equal to

$$\begin{aligned} & \left(-\frac{i_1}{i} + 1\right)^{-1} \log(q) \left( q^{-1+\frac{1}{i}} \int_{\frac{1}{q-1+i}}^1 \left(\frac{1}{z} - 1\right)^{\frac{1}{i}} dz - q^{-1+\frac{1}{i_1}} \int_{\frac{1}{q-1+i_1}}^1 \left(\frac{1}{z} - 1\right)^{\frac{1}{i_1}} dz \right) \tag{B7} \\ & = \left(-\frac{i_1}{i} + 1\right)^{-1} \left( \underbrace{q^{-1+\frac{1}{i}} \log(q) \int_0^{q-1} \frac{z'^{\frac{1}{i}}}{(z'+1)^2} dz'}_{\mathfrak{D}.III.1} - \underbrace{q^{-1+\frac{1}{i_1}} \log(q) \int_0^{q-1} \frac{z'^{\frac{1}{i_1}}}{(z'+1)^2} dz'}_{\mathfrak{D}.III.2} \right). \end{aligned}$$

Since  $i, i_1 > 1$ , the integrals in  $\mathfrak{D}.III.1$  and in  $\mathfrak{D}.III.2$  are uniformly bounded for  $q > 0$ . The rate of divergence of  $\mathfrak{D}.III$  is therefore  $-\Theta\left(-q^{1-\frac{1}{i}} \log(q)\right)$ . Through a similar approach, we note that  $\mathfrak{D}.IV$  is equal to

$$\left(-\frac{i_1}{i} + 1\right)^{-1} \left( \underbrace{q^{-1+\frac{1}{i}} \int_0^{q-1} \frac{z'^{\frac{1}{i}} \log(z')}{(z'+1)^2} dz'}_{\mathfrak{D}.IV.1} - \underbrace{q^{-1+\frac{1}{i_1}} \int_0^{q-1} \frac{z'^{\frac{1}{i_1}} \log(z')}{(z'+1)^2} dz'}_{\mathfrak{D}.IV.2} \right).$$

The rate of divergence of  $\mathfrak{D}.IV$  is  $\Theta\left(q^{1-\frac{1}{i}}\right)$  because the integrals in  $\mathfrak{D}.IV.1$  and  $\mathfrak{D}.IV.2$  are uniformly bounded for  $q > 0$  since  $i, i_1 > 1$ . Lastly, through integration by parts we obtain that  $\mathfrak{D}.V$  is equal to

$$\begin{aligned} & \left(-\frac{i_1}{i} + 1\right)^{-1} q^{-1+\frac{1}{i}} \log\left(q^{-\frac{1}{3i_1}}\right) \int_{\frac{1}{q-1+i}}^1 \left(\frac{1}{z} - 1\right)^{\frac{1}{i}} dz \\ & - \left(-\frac{i_1}{i} + 1\right)^{-2} q^{-1+\frac{1}{i}} \int_{\frac{1}{q-1+i}}^1 \left(\frac{1}{z} - 1\right)^{\frac{1}{i}} dz \\ & - \left(-\frac{i_1}{i} + 1\right)^{-1} q^{-1+\frac{1}{i_1}} \int_{\frac{1}{q-1+i_1}}^1 \left(\frac{1}{z} - 1\right)^{\frac{1}{i_1}} \log\left(\left(\frac{1}{z} - 1\right)^{\frac{1}{i_1}} q^{\frac{2}{3i_1}}\right) dz \\ & + \left(-\frac{i_1}{i} + 1\right)^{-2} q^{-1+\frac{1}{i_1}} \int_{\frac{1}{q-1+i_1}}^1 \left(\frac{1}{z} - 1\right)^{\frac{1}{i_1}} dz \tag{B8} \\ & = -\left(-\frac{i_1}{i} + 1\right)^{-2} \underbrace{q^{-1+\frac{1}{i}} \int_0^{q-1} \frac{z'^{\frac{1}{i}}}{(z'+1)^2} dz'}_{\mathfrak{D}.V.1} + \left(-\frac{i_1}{i} + 1\right)^{-2} \underbrace{q^{-1+\frac{1}{i_1}} \int_0^{q-1} \frac{z'^{\frac{1}{i_1}}}{(z'+1)^2} dz'}_{\mathfrak{D}.V.2} \\ & - \left(-\frac{i_1}{i} + 1\right)^{-1} \frac{1}{3i_1} \underbrace{q^{-1+\frac{1}{i}} \log(q) \int_0^{q-1} \frac{z'^{\frac{1}{i}}}{(z'+1)^2} dz'}_{\mathfrak{D}.V.3} - \left(-\frac{i_1}{i} + 1\right)^{-1} \frac{2}{3i_1} \underbrace{q^{-1+\frac{1}{i_1}} \log(q) \int_0^{q-1} \frac{z'^{\frac{1}{i_1}}}{(z'+1)^2} dz'}_{\mathfrak{D}.V.4} \\ & - \left(-\frac{i_1}{i} + 1\right)^{-1} \frac{1}{i_1} \underbrace{q^{-1+\frac{1}{i_1}} \int_0^{q-1} \frac{z'^{\frac{1}{i_1}} \log(z')}{(z'+1)^2} dz'}_{\mathfrak{D}.V.5}. \end{aligned}$$

The rate of divergence of  $\mathfrak{D}.V$  is  $\Theta\left(-q^{-1+\frac{1}{i}} \log(q)\right)$ , since the integrals in (B8) are uniformly bounded for  $q > 0$ . Overall, the rate assumed by  $\mathfrak{D}$  is

$$\Theta\left(-q^{1-\frac{1}{i}} \log(q)\right) - \Theta\left(q^{1-\frac{1}{i}}\right) + \Theta\left(-q^{-1+\frac{1}{i}} \log(q)\right) = \Theta\left(-q^{-1+\frac{1}{i}} \log(q)\right).$$

We find the rate of divergence for the upper bound in the case  $i_3 = i_2 > i_1 > 1$  given by

$$\Theta\left((-p)^{-1+\frac{1}{i_2}}\right) + \Theta\left(-(-p)^{-1+\frac{1}{i_3}} \log(-p)\right) = \Theta\left(-(-p)^{-1+\frac{1}{i_3}} \log(-p)\right).$$

◆ Scaling law of  $\mathfrak{D}$  in Case 4. We suppose now that  $i_3 = i_2 = i_1 > 1$ . We trace the previous case until equation (B6) and label  $i = i_3 = i_2 = i_1$ . Therefore,  $\mathfrak{D.III}$  is equal to

$$\begin{aligned}
 & q^{-1+\frac{1}{i}} \log(q) \int_{\frac{1}{q^{-1+i}}}^1 \int_{\left(\frac{1}{z}-1\right)^{\frac{1}{i}} q^{\frac{2}{3i}}}^{q^{-\frac{1}{3i}}} \left(\frac{1}{z}-1\right)^{\frac{1}{i}} y_1^{-1} dy_1 dz \\
 &= -\frac{1}{i} q^{-1+\frac{1}{i}} \log(q) \left( \log(q) \int_{\frac{1}{q^{-1+i}}}^1 \left(\frac{1}{z}-1\right)^{\frac{1}{i}} dz + \int_{\frac{1}{q^{-1+i}}}^1 \left(\frac{1}{z}-1\right)^{\frac{1}{i}} \log\left(\frac{1}{z}-1\right) dz \right) \quad (\text{B9}) \\
 &= -\frac{1}{i} q^{-1+\frac{1}{i}} \log^2(q) \underbrace{\int_0^{q^{-1}} \frac{z'^{\frac{1}{i}}}{(z'+1)^2} dz'}_{\mathfrak{D.III.3}} - \frac{1}{i} q^{-1+\frac{1}{i}} \log(q) \underbrace{\int_0^{q^{-1}} \frac{z'^{\frac{1}{i}} \log(z')}{(z'+1)^2} dz'}_{\mathfrak{D.III.4}}.
 \end{aligned}$$

Since  $i > 1$ , the integrals in the right-hand side of (B9) are uniformly bounded for any  $q > 0$ . Therefore the rate of divergence of  $\mathfrak{D.III}$  is  $-\Theta\left(q^{-1+\frac{1}{i}} \log^2(q)\right)$ . Similarly, the summand  $\mathfrak{D.IV}$  assumes value

$$\begin{aligned}
 & q^{-1+\frac{1}{i}} \int_{\frac{1}{q^{-1+i}}}^1 \int_{\left(\frac{1}{z}-1\right)^{\frac{1}{i}} q^{\frac{2}{3i}}}^{q^{-\frac{1}{3i}}} \left(\frac{1}{z}-1\right)^{\frac{1}{i}} \log\left(\frac{1}{z}-1\right) y_1^{-1} dy_1 dz \\
 &= -\frac{1}{i} q^{-1+\frac{1}{i}} \left( \log(q) \int_{\frac{1}{q^{-1+i}}}^1 \left(\frac{1}{z}-1\right)^{\frac{1}{i}} \log\left(\frac{1}{z}-1\right) dz + \int_{\frac{1}{q^{-1+i}}}^1 \left(\frac{1}{z}-1\right)^{\frac{1}{i}} \log^2\left(\frac{1}{z}-1\right) dz \right) \quad (\text{B10}) \\
 &= -\frac{1}{i} q^{-1+\frac{1}{i}} \log(q) \underbrace{\int_0^{q^{-1}} \frac{z'^{\frac{1}{i}} \log(z')}{(z'+1)^2} dz'}_{\mathfrak{D.IV.3}} - \frac{1}{i} q^{-1+\frac{1}{i}} \underbrace{\int_0^{q^{-1}} \frac{z'^{\frac{1}{i}} \log^2(z')}{(z'+1)^2} dz'}_{\mathfrak{D.IV.4}}.
 \end{aligned}$$

Again, since  $i > 1$ , the integrals in the right-hand side of (B10) are uniformly bounded for any  $q > 0$  and the rate of divergence of  $\mathfrak{D.IV}$  is in this case  $\Theta\left(-q^{-1+\frac{1}{i}} \log(q)\right)$ . Lastly, the summand  $\mathfrak{D.V}$  is equal to

$$\begin{aligned}
 & q^{-1+\frac{1}{i}} \int_{\frac{1}{q^{-1+i}}}^1 \int_{\left(\frac{1}{z}-1\right)^{\frac{1}{i}} q^{\frac{2}{3i}}}^{q^{-\frac{1}{3i}}} \left(\frac{1}{z}-1\right)^{\frac{1}{i}} y_1^{-1} \log(y_1) dy_1 dz \\
 &= \frac{1}{2} q^{-1+\frac{1}{i}} \log^2\left(q^{-\frac{1}{3i}}\right) \int_{\frac{1}{q^{-1+i}}}^1 \left(\frac{1}{z}-1\right)^{\frac{1}{i}} dz - \frac{1}{2} q^{-1+\frac{1}{i}} \int_{\frac{1}{q^{-1+i}}}^1 \left(\frac{1}{z}-1\right)^{\frac{1}{i}} \log^2\left(\left(\frac{1}{z}-1\right)^{\frac{1}{i}} q^{\frac{2}{3i}}\right) dz \\
 &= -\frac{1}{6i^2} q^{-1+\frac{1}{i}} \log^2(q) \int_{\frac{1}{q^{-1+i}}}^1 \left(\frac{1}{z}-1\right)^{\frac{1}{i}} dz - \frac{2}{3i^2} q^{-1+\frac{1}{i}} \log(q) \int_{\frac{1}{q^{-1+i}}}^1 \left(\frac{1}{z}-1\right)^{\frac{1}{i}} \log\left(\frac{1}{z}-1\right) dz \\
 &\quad - \frac{1}{2i^2} q^{-1+\frac{1}{i}} \int_{\frac{1}{q^{-1+i}}}^1 \left(\frac{1}{z}-1\right)^{\frac{1}{i}} \log^2\left(\frac{1}{z}-1\right) dz \quad (\text{B11}) \\
 &= -\frac{1}{6i^2} q^{-1+\frac{1}{i}} \log^2(q) \underbrace{\int_0^{q^{-1}} \frac{z'^{\frac{1}{i}}}{(z'+1)^2} dz'}_{\mathfrak{D.V.6}} - \frac{2}{3i^2} q^{-1+\frac{1}{i}} \log(q) \underbrace{\int_0^{q^{-1}} \frac{z'^{\frac{1}{i}} \log(z')}{(z'+1)^2} dz'}_{\mathfrak{D.V.7}} \\
 &\quad - \frac{1}{2i^2} q^{-1+\frac{1}{i}} \underbrace{\int_0^{q^{-1}} \frac{z'^{\frac{1}{i}} \log^2(z')}{(z'+1)^2} dz'}_{\mathfrak{D.V.8}}.
 \end{aligned}$$

Since  $i > 1$ , the integrals in the right-hand side of (B11) are uniformly bounded for any  $q > 0$  and the rate of divergence of  $\mathfrak{D}.V$  is in this case  $-\Theta\left(q^{-1+\frac{1}{i}} \log^2(q)\right)$ . Observing (B6), (B9) and (B11), we note that the leading terms of  $\mathfrak{D}$  are  $\frac{2}{3i^2}\mathfrak{D}.III.3$  and  $-\frac{1}{6i^2}\mathfrak{D}.V.6$ . Hence  $\mathfrak{D}$  is characterised by the same rate of divergence as

$$\frac{2}{3i^2}\mathfrak{D}.III.3 - \frac{1}{6i^2}\mathfrak{D}.V.6 = \frac{1}{2i^2}q^{-1+\frac{1}{i}} \log^2(q) \int_0^{q^{-1}} \frac{z'^{\frac{1}{i}}}{(z'+1)^2} dz' = \Theta\left(q^{-1+\frac{1}{i}} \log^2(q)\right).$$

Combining both summands  $\mathfrak{C}$  and  $\mathfrak{D}$ , we obtain the rate of the upper bound as

$$\Theta\left(-(-p)^{-1+\frac{1}{2}} \log(-p)\right) + \Theta\left((-p)^{-1+\frac{1}{i}} \log^2(-p)\right) = \Theta\left((-p)^{-1+\frac{1}{i}} \log^2(-p)\right)$$

for  $i_3 = i_2 = i_1 > 1$ .

◆ **Scaling law of  $\mathfrak{D}$  in Case 5.** In the next case, we consider  $i_3 > i_2 > i_1 = 1$ . We can follow the same steps as in the computation of the scaling law of  $\mathfrak{D}$  in Case 1, but we note that the integrals in  $\mathfrak{D}.I.2$  and  $\mathfrak{D}.II.2$  diverge as  $\Theta(\log(q^{-1}))$  due to (A7). The rate of divergence of  $\mathfrak{D}$  is therefore

$$\Theta\left(q^{-1+\frac{1}{3}}\right) - \Theta(-\log(q)) - \Theta\left(q^{-1+\frac{1}{2}}\right) + \Theta(-\log(q)) = \Theta\left(q^{-1+\frac{1}{3}}\right)$$

and the rate of the upper bound in the case  $i_3 > i_2 > i_1 = 1$  is

$$\Theta\left((-p)^{-1+\frac{1}{2}}\right) + \Theta\left((-p)^{-1+\frac{1}{3}}\right) = \Theta\left((-p)^{-1+\frac{1}{3}}\right).$$

◆ **Scaling law of  $\mathfrak{D}$  in Case 6.** We assume that  $i_3 > i_2 = i_1 = 1$  and proceed as in the previous case as we prove that the rate of divergence of  $\mathfrak{D}.I$  is

$$\Theta\left(q^{-1+\frac{1}{3}}\right) - \Theta(-\log(q)) = \Theta\left(q^{-1+\frac{1}{3}}\right).$$

We can then follow the same approach as in the computation of the scaling law of  $\mathfrak{D}$  in Case 2 and study the summands in (B5). Inserting  $i_2 = i_1 = i = 1$ , we know, from (A7), that the rate of divergence assumed by  $\mathfrak{D}.II.3$  is  $-\Theta(\log^2(q))$ . We also know, from (C1) in Appendix C, that the rate of  $\mathfrak{D}.II.4$  is  $\Theta(\log^2(q))$ . Hence, we can state that  $\mathfrak{D} = \Theta\left(q^{-1+\frac{1}{3}}\right)$ , and in the case  $i_3 > i_2 = i_1 = 1$  that the rate of divergence of the upper bound is

$$\Theta(\log^2(-p)) + \Theta\left((-p)^{-1+\frac{1}{3}}\right) = \Theta\left((-p)^{-1+\frac{1}{3}}\right).$$

◆ **Scaling law of  $\mathfrak{D}$  in Case 7.** We now consider  $i_3 = i_2 > i_1 = 1$ . We follow the same approach employed in the computation of the scaling law of  $\mathfrak{D}$  in Case 3 and set  $i_3 = i_2 = i$ . We obtain that, due to (A7) and (C1),

$$\begin{aligned} \mathfrak{D}.III.1 &= -\Theta\left(-q^{1-\frac{1}{i}} \log(q)\right) & \mathfrak{D}.III.2 &= -\Theta(\log^2(q)) & \mathfrak{D}.IV.1 &= \Theta\left(q^{1-\frac{1}{i}}\right) & , \\ \mathfrak{D}.IV.2 &= \Theta(\log^2(q)) & \mathfrak{D}.V.1 &= \Theta\left(q^{1-\frac{1}{i}}\right) & \mathfrak{D}.V.2 &= \Theta(-\log(q)) & , \\ \mathfrak{D}.V.3 &= -\Theta\left(-q^{1-\frac{1}{i}} \log(q)\right) & \mathfrak{D}.V.4 &= -\Theta(\log^2(q)) & \mathfrak{D}.V.5 &= \Theta(\log^2(q)) & . \end{aligned}$$

The rate of divergence of  $\mathfrak{D}$  is hence

$$\begin{aligned} &\Theta\left(-q^{1-\frac{1}{i}} \log(q)\right) - \Theta(\log^2(q)) - \Theta\left(q^{1-\frac{1}{i}}\right) + \Theta(\log^2(q)) - \Theta\left(q^{1-\frac{1}{i}}\right) \\ &+ \Theta(-\log(q)) + \Theta\left(-q^{1-\frac{1}{i}} \log(q)\right) + \Theta(\log^2(q)) - \Theta(\log^2(q)) = \Theta\left(-q^{1-\frac{1}{i}} \log(q)\right). \end{aligned}$$

Combining the results on the scaling law of  $\mathfrak{C}$  and of  $\mathfrak{D}$ , we observe that the rate of divergence of the upper bound is

$$\Theta\left((-p)^{-1+\frac{1}{2}}\right) + \Theta\left(-(-p)^{-1+\frac{1}{i}} \log(-p)\right) = \Theta\left(-(-p)^{-1+\frac{1}{i}} \log(-p)\right),$$

for  $i_3 = i_2 > i_1 = 1$ .

◆ Scaling law of  $\mathfrak{D}$  in Case 8. The last case for which we evaluate  $\mathfrak{D}$  assumes  $i_3 = i_2 = i_1 = 1$ . Following the same steps of the computation of the scaling law of  $\mathfrak{D}$  in Case 4, we obtain (B9), (B10) and (B11). We know, from (A7) and (C3) in Appendix C, that  $\mathfrak{D}.$ III.3,  $\mathfrak{D}.$ IV.4,  $\mathfrak{D}.$ V.6, and  $\mathfrak{D}.$ V.8 diverge with rate  $\Theta(-\log^3(q))$  and that  $\mathfrak{D}.$ III.4,  $\mathfrak{D}.$ IV.3,  $\mathfrak{D}.$ V.7 as  $-\Theta(-\log^3(q))$ . From (A7), (C2) and (C3), we get the rate of divergence of the summand  $\mathfrak{D}$  as

$$\begin{aligned} & \frac{2}{3}\mathfrak{D}.$$
III.3 +  $\frac{2}{3}\mathfrak{D}.$ III.4 +  $\mathfrak{D}.$ IV.3 +  $\mathfrak{D}.$ IV.4 -  $\frac{1}{6}\mathfrak{D}.$ V.6 -  $\frac{2}{3}\mathfrak{D}.$ V.7 -  $\frac{1}{2}\mathfrak{D}.$ V.8 \\ &= \left(\frac{2}{3} - \frac{2}{3} \frac{1}{2} - \frac{1}{2} + \frac{1}{3} - \frac{1}{6} + \frac{2}{3} \frac{1}{2} - \frac{1}{2} \frac{1}{3}\right) \Theta(-\log^3(q)) = \Theta(-\log^3(q)) \end{aligned}

Conclusively, in the case  $i_3 = i_2 = i_1 = 1$  we find that  $\langle g, V_\infty g \rangle$  has an upper bound with rate of divergence

$$\Theta(\log^2(-p)) + \Theta(-\log^3(-p)) = \Theta(-\log^3(-p)) .$$

□

### Appendix C

For  $q > 0$  and  $m \in \mathbb{N} \cup \{0\}$ ,

$$\int_0^{q^{-1}} \frac{z' \log^m(z')}{(z' + 1)^2} dz' = \Theta((-\log(q))^{m+1}) \tag{C1}$$

holds true by considering

$$\lim_{q \rightarrow 0^+} \int_0^{q^{-1}} \frac{z' \log^m(z')}{(z' + 1)^2} dz' = \int_0^n \frac{z' \log^m(z')}{(z' + 1)^2} dz' + \lim_{q \rightarrow 0^+} \int_n^{q^{-1}} \frac{z' \log^m(z')}{(z' + 1)^2} dz' ,$$

with  $n > 0$ . Whereas the first integral is finite for any finite  $n > 0$ , we find that, in the limit  $z' \rightarrow +\infty$ ,  $\frac{z' \log^m(z')}{(z' + 1)^2}$  behaves equivalently to  $\frac{\log^m(z')}{z'}$  since

$$\lim_{z' \rightarrow \infty} \frac{(z' + 1)^{-2} z' \log^m(z')}{z'^{-1} \log^m(z')} = 1 . \tag{C2}$$

We then study the integral

$$\int_n^{q^{-1}} \frac{\log^m(z')}{z'} dz' = \left[ \frac{1}{m+1} \log^{m+1}(z') \right]_n^{q^{-1}} = \frac{1}{m+1} \log^{m+1}(q^{-1}) - \frac{1}{m+1} \log^{m+1}(n) ,$$

which concludes the proof.

Lastly, we note that

$$\lim_{q \rightarrow 0^+} \frac{1}{\frac{1}{m+1} \log^{m+1}(q^{-1})} \int_0^{q^{-1}} \frac{z' \log^m(z')}{(z' + 1)^2} dz' = 1 . \tag{C3}$$